Renewable and Sustainable Energy Reviews 90 (2018) 223–247

Contents lists available at ScienceDirect

Renewable and Sustainable Energy Reviews

journal homepage: www.elsevier.com/locate/rser

A review of the hydrothermal carbonization of biomass waste for hydrochar formation: Process conditions, fundamentals, and physicochemical properties

Tengfei Wang[a,b], Yunbo Zhai[a,b,*], Yun Zhu[c], Caiting Li[a,b], Guangming Zeng[a,b]

[a] College of Environmental Science and Engineering, Hunan University, Changsha 410082, PR China
[b] Key Laboratory of Environmental Biology and Pollution Control (Hunan University), Ministry of Education, Changsha 410082, PR China
[c] Office of Scientific R&D, Hunan University, Changsha 410082, PR China

ARTICLE INFO

Keywords:
Biomass
Hydrothermal carbonization
Hydrochar
Characterization
Mechanism

ABSTRACT

Hydrothermal carbonization (HTC) is a thermochemical conversion technique which is attractive due to its ability to transform wet biomass into energy and chemicals without predrying. The solid product, known as hydrochar, has received attention because of its ability to prepare precursors of activated carbon in wastewater pollution remediation, soil remediation applications, solid fuels, and other carbonaceous materials. Besides the generally lignocellulose biomass used as sustainable feedstock, HTC has been applied to a wide range of derived waste, including sewage sludge, algae, and municipal solid waste to solve practical problems and generate desirable carbonaceous products. This review presented the critical hydrothermal parameters of HTC, including temperature, residence time, heating rate, reactant concentration, and aqueous quality. The chemical reaction mechanisms involved in the formation of hydrochar derived from single components and representative feedstock, lignocellulose, and sludge termed as N-free and N-rich biomass, were elucidated and summarized to better understand the hydrochar formation process. Specifically, hydrochar physicochemical characteristics such as surface chemistry and structure were investigated. Current knowledge gaps, and new perspectives with corresponding recommendations were provided to further exploit the great potential of the HTC technique and more practical applications for hydrochar in the future.

1. Introduction

Biomass represents the biological materials from plants or animals and their derived waste and residues [1]. The utilization of waste biomass as a sustainable resource has been recognized by society mainly due to potential reductions in greenhouse gas emissions (GHGs) [2,3]. It is possible that near zero GHG emissions can be achieved by balancing plant biomass production and utilization in the future [4]. Needless to say, it is critical to search for technologies that are sustainable, non-polluting, and effective. In addressing these concerns, diverse methods of biomass utilization for energy recovery have been found to be economically viable and environmentally friendly. Biomass such as lignocellulose, sewage sludge (SS), and municipal solid waste (MSW) are considered to be an abundant and renewable resource which can be converted into solid, liquid, and gaseous form using biochemical, physicochemical, and thermochemical technologies [1,5,6]. However, there are disadvantages to biomass as a sustainable resource that urgently need to be overcome; for example, its high moisture, low energy content, heterogeneity, low density, and presence of contaminants. In previous studies, common biomass utilization approaches have included pyrolysis, biological conversion, densification to a solid fuel, and hydrothermal processes [7–10]. Pyrolysis is faced with the main obstacle that the high moisture content of biomass requires high heat for vaporization [9]. Moreover, biological conversion processes such as fermentation and anaerobic digestion, despite consuming low energy, require longer timeframes as compared to thermal processes [11]. Subsequently, much attention has centered on hydrothermal conversion processes which have been shown to be more cost-effective as compared to conventional thermal drying [12]. Hydrothermal processes for biomass utilization have both advantages and disadvantages, and these are summarized in Table 1. Of the hydrothermal processes, hydrothermal carbonization (HTC), discovered in 1913 by Bergius [13] was found to mimic the natural process of coal formation that converted cellulose into coal like materials. This artificial coalification process was later re-discovered and has been variously referred to as hot compressed water treatment, subcritical water treatment, wet

* Corresponding author at: College of Environmental Science and Engineering, Hunan University, Changsha 410082, PR China.
E-mail address: ybzhai@hnu.edu.cn (Y. Zhai).

https://doi.org/10.1016/j.rser.2018.03.071
Received 25 December 2016; Received in revised form 13 February 2018; Accepted 22 March 2018
1364-0321/

Table 1
Brief approaches of biomass utilization techniques and advantages or disadvantages.

Approaches of biomass utilization	Advantages	Disadvantages	Approach and objective
Pyrolysis	High efficiency and flexibility	Not suitable for high moisture biomass waste	Slow or fast pyrolysis producing biochar, bio-oil and gases like CO, CO_2, CH_4 and H_2
Hydrothermal process	It can be directly applied to biomass with high moisture	Difficult to collect the products and high requirements for equipment	Carbonization, liquefaction and gasification producing hydrochar, bio-oil and gas
Biological conversion	Lower process energy requirements	Period is long	Fermentation or anaerobic digestion producing bio-ethanol and bio-gas
Densified as solid fuel	Lower transportation costs	Energy content is low	Pelletization for fuel pellet or briquette production

torrefaction, and hydrothermal treatment. In recent years, the unwanted solid residue during hydrothermal gasification and liquidation, has received increasing attention [14].

During the HTC process, raw biomass is converted into a lignite-like solid product that is significantly affected by the medium [15]. Because wet biomass requires no predrying prior to HTC, it has been successfully introduced and practically applied. Moreover, water is an inexpensive, environmentally benign, and nontoxic media [16]. Generally, the HTC process occurs at relatively low temperatures (180 − 250 °C) and under autogenous pressure that lowers both the oxygen and hydrogen content of the feedstock through dehydration and decarboxylation [17]. This process is governed by hydrothermal parameters such as residence time and temperature, which determine the reaction severity and degree of coalification of the raw biomass [18,19]. The solid residue derived from the HTC process, defined as hydrochar in this review, exhibits high hydrophobic and friable properties, and hence, is easily separated from the liquid product. The hydrochar demonstrates superior performance relative to the raw biomass in terms of higher mass and energy density, better dewaterability, and improved combustion performance as a solid fuel [9]. Based on the different kinds of biomass used, hydrochar has been widely used for carbon sequestration, soil amelioration, bioenergy production, and wastewater pollution remediation [20]. Unlike the solid products, liquid products require fractionation by extraction when used for bio-oil production. Moreover, research has indicated that the liquid products from hydrothermal treatment are biodegradable on account of their high organic substance [21–23]. Hydrochar has been demonstrated as a high value, carbon-rich material after undergoing hydrothermal treatment to reduce its hydrogen and oxygen content [17]. Importantly, the utilization of these carbon-rich materials is in many aspects a sustainable way to mitigate anthropogenic CO_2 [24]. The sustainability benefits of hydrochar production and its potential applications are summarized in Fig. 1. Firstly, green plants remove CO_2 by photosynthesis; through the HTC process, this CO_2 is bonded to the final carbonaceous structure of the hydrochar, representing an effective approach to diminish CO_2 from the carbon cycle. Furthermore, the bio-oil and hydrochar produced during the HTC process can be employed as biofuel, reducing dependency on fossil fuels and further offsetting CO_2 emissions. Meanwhile, large amounts of human derivative waste biomass including SS, feces, MSW, and lignocellulose can be converted into hydrochar. In terms of carbon migration, the production of hydrochar from human waste can be regarded as strengthening the immobilization of CO_2 from a recalcitrant form of carbon carrier.

In recent years, the potential benefits and applications of hydrochar have received significant attention, both in terms of producing functionalized carbon materials and the various potential applications of hydrochar in the field of energy storage and environmental protection. Since 2009, there has been rapid growth in the number of publications related to the production and application of hydrochar. For example, Libra et al. [25] and Reza et al. [26] summarized the technical and climate change aspects of hydrochar production and discussed the application of hydrochar in soil remediation. Kambo et al. [9] and Zhao et al. [27], respectively, reviewed the characteristics of hydrochar production and highlighted the benefits of waste biomass derived hydrochar as a clean solid fuel from HTC. Current commercial and large-scale applications of the HTC process were reviewed by Okajima et al. [28]. Jain et al. [29] reviewed hydrochar formation mechanisms and identified a high density of oxygenated functional group products in the process. To date, few reviews have focused on detailing hydrochar formation mechanisms, especially in terms of available single components. In particular, there is a need to critically and comprehensively understand the complex conversion of waste biomass during the HTC process, and to explore the research advances, challenges, and future opportunities of thoroughly utilizing the superiority of hydrochar. In this review, we discuss the critical hydrothermal parameters in the HTC process; mechanisms of hydrochar formation in response to single components and typical biomass including lignocellulose and SS (N-free and N-rich biomass, respectively); and the physical, chemical, and structural characteristics of hydrochar. Additionally, we provide some perspective on future research opportunities and applications of hydrochar.

2. Production of hydrochar

2.1. HTC process

The HTC process occurs in the subcritical region as shown in Fig. 2. It is widely known that the characteristics of water change dramatically under subcritical conditions. Temperature increases below 374 °C decrease the dielectric constant, weakening water's hydrogen bonds and producing high ionization constants, which enhance the dissociation of water into acidic hydronium ions (H_3O^+) and basic hydroxide ions (OH^-) [30–32]. Furthermore, the subcritical water itself can boast a sufficiently higher H^+ concentration as compared to liquid water, which is an excellent medium for the acid-catalyzed reaction of organic compounds without added acid [30,33]. Under different temperatures, water properties change dramatically and the field of application for hydrothermal processes are shown in During HTC, the water contained in the biomass or supplied to the process is an excellent solvent and reaction medium [25]. Conditions are mildly controlled at relatively low temperatures (180–250 °C) under autogenous pressure maintained for a specified residence time [17,25]. In recent studies, various feedstocks were selected for HTC, ranging from model substances to actual feedstock including cellulose [36,37], glucose [37], agricultural residue [38], animal manures [39], food waste [40,41], MSW [42], SS [43,44], and aquaculture and algal residues [45]. It is apparent that the HTC process is not restricted to traditional lignocellulosic biomass; feedstocks can be more complex, and these renewable feedstocks represent large quantities of organic matter that require proper treatment to limit pollution of the environment. The products of HTC mainly consist of three components: solid, aqueous solution (bio-oil mixed with water), and a small volume of gas (mainly CO_2). The distribution and properties of these products is heavily influenced by the feedstock and process conditions [46,47]. Solid residue is regarded as the main product of HTC; it can be easily separated from the suspension due to its high hydrophobicity and homogeneous properties [48]. Furthermore,

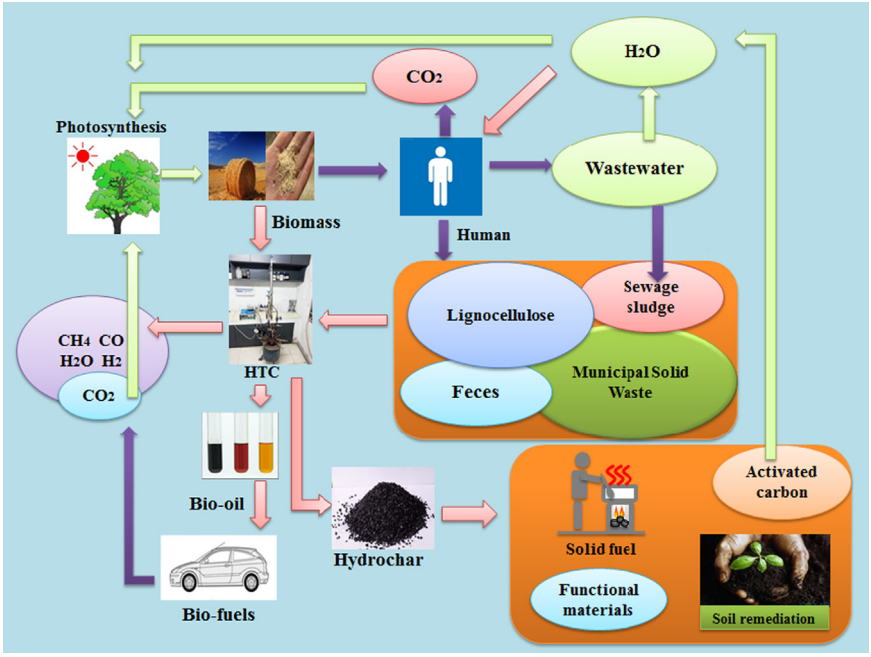

Fig. 1. Schematic illustration of sustainable concepts regarding hydrochar production, applications, and impact on global climate.

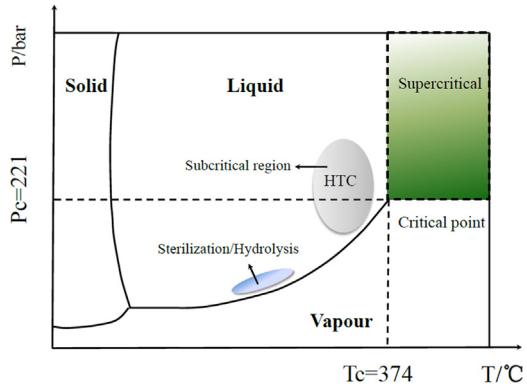

Fig. 2. The water properties changes under different temperatures and the application field of hydrothermal processes from [34,35].

hydrothermal parameters can produce great diversity in the physico-chemical properties of hydrochar. To fully explore the extraordinary properties and the potential applications of hydrochar, it is necessary to understand the critical process parameters governing HTC and the mechanisms of the hydrochar formation process.

2.2. Effect of process parameters

2.2.1. Temperature

Temperature represents a critical factor in the HTC process because it is a main determinant of the water properties which cause ionic reactions occur in the subcritical region. Above the critical point, the reaction mechanism shifts from ionic to free-radical reactions in the supercritical water region [30]. However, in ionic dominated HTC reactions, the increase in temperature alters the water viscosity, allowing for easier penetration into porous media, and thus, further degrading the biomass [17]. Furthermore, when the temperature exceeds the activation energy, bond cessation commences in the biomass macromolecular organics [49].

Temperatures approaching a certain reaction intensity have a decisive influence on the hydrolysis reaction of biomass, and the higher temperatures can lead to dehydration, decarboxylation, and condensation simultaneously. When the temperature is not sufficient to break up the major components of the biomass, a pyrolysis-like process at the lower temperatures described above is likely to happen as opposed to the monomers reaction during the homogeneous reaction. For example, temperatures of 200 °C showed limited degradation of cellulose leading to a partial pyrolysis-like process [50]. Unlike the solid–solid conversion, the use of high temperatures with sufficient residence time may lead to a high degree of intermediate dissolution and subsequent conversion through polymerization, forming secondary char, which dominates the mechanisms of hydrochar formation [51]. Variations resulting from temperature differences can also be demonstrated by the elemental composition of hydrochar products, and analysis of Van Krevelen diagrams characterizing the evolution of the H/C and O/C atomic ratios, which will discussed be in the following sections [52]. Sevilla et al. [53] reported that an increase in the temperature of HTC from 230° to 250°C caused a decrease in the O/C and H/C atomic ratios, suggesting that increased temperatures improved the degree of condensation of the hydrochar. Parshetti et al. [54] used empty palm fruit bunches as lignocellulosic material and employed temperatures of 150 °C, 250 °C, and 350 °C. They found that the H/C and O/C atomic ratios of hydrochar decreased steadily with temperature. Similar tendencies were also observed for the HTC of other biomass such as starch, MSW, and SS [55–57]. However, while the polymerization rate of the fragments depended heavily on the temperature, there was a lack of detailed data on the process [17].

Generally, the distribution of the products is heavily influenced by temperature. As temperatures increase, the hydrochar yields of bio-oil and gaseous products decrease. However, Ying et al. [36] found that when the temperature was increased above 200 °C, the solid product of cellulose decreased due to improved decomposition by the fragmentation of large molecules into components including liquids or incondensable low molecular gas. The main gas products were CO, CO_2, H_2, and CH_4, with CO_2 having the highest fraction. When the temperature increased from 250° to 350°C, the yield of CH_4 increased from 1.92% to 4.89%, while the H_2 concentration increased to approximately 10.6% [36]. Higher temperatures would also lead to the secondary decomposition of the solid residue, resulting in the further conversion of condensable products to incondensable gas products. Hoekman et al. [58] found the mass yield of hydrochar from lignocellulose decreased

from 69.1% to 50.1% when the temperature increased from 215° to 255°C, predominantly due to the conversion to total organic carbon (TOC) containing sugars and organic acids in the liquid products. However, higher temperatures (> 295 °C) would lead to lower TOC with low sugar content and a high organic acid content. In our research, when the SS HTC reaction temperature increased from 180° to 300°C, the hydrochar yield declined from 66.18% to 53.00%, and results indicated that the degree of condensation was promoted by improving the temperature during the HTC process. This decrease was attributed to dehydration, decarboxylation, and volatile matter reduction; with oxygen and hydrogen contents decreasing when high temperatures were used [59]. While high temperatures lead to a reduction in solid residue, hydrochar energy densification was observed in many studies, reinforcing hydrochar as a good source of solid fuel.

2.2.2. Residence time

Residence time is an important factor in hydrochar formation because a long residence time enhances reaction severity. Compared with the temperature, the residence time had a similar yet smaller effect on solid product recovery; solid hydrochar content was high when residence time was short and decreased as residence time increased. A long residence time resulted in the polymerization of fragments solved in the liquid phase that led to the formation of secondary hydrochar with a polyaromatic structure [60,61]. For lignocellulose materials, secondary hydrochar formation depended heavily on the residence time, because dissolved monomers required extensive polymerization. Conversely, non-dissolved monomers may have a greater dependence on temperature. Based on this finding, we expect that controlling the residence time determines the degree of polymerization of the soluble monomers during HTC, and provides an opportunity for the pyrolysis-like process to be performed. High condensation polymers showed the same behavior with increased residence time that was observed with increased temperature; that is, coalification due to a decrease in O/C and H/C. However, the coalification process may differ because residence time enhances the reaction by increasing the formation of intermediate products. In research by Gao et al. [62], increasing the residence time from 30 min to 24 h at 240 °C resulted in different surface characteristics on hydrochar from water hyacinth. Results showed that a short residence time for HTC will result in cracks and trenches on the hydrochar surface, with no microspheres or carbon microspheres formed until the residence time exceeds six hours. Residence times exceeding 24 h resulted in aggregations of the microspheres on the surface of hydrochar [62]. The residence time controls the degree of decomposition of the raw materials at a certain temperature by determining the hydrolysis and polymerization of the monomers, resulting in different hydrochar textures after the formation of microspheres. This factor not only governs the means of dispersion or aggregation of the microspheres, but also impacts the diameter of the microspheres. Sevilla et al. [56] found that glucose hydrothermally carbonized at 170 °C, and residence times of 4.5 and 15 h showed different mean microparticle diameters. A similar result was found by Romero-Anaya et al. [63], who showed that longer residence times (12–48 h) determined the morphology of the hydrochar particles, which were not well defined as spherical carbons, using both glucose and sucrose as starting materials **(**Fig. 3**)**. Thus, increasing residence time exhibits a similar effect to increasing temperature by enhancing the aggregation of microspheres on the hydrochar. Falco et al. [64] showed that hydrochar derived from glucose exhibited an average particle hydrodynamic radius of 685 nm at 260 °C and a radius of 474 nm at 160 °C. Hence, we conclude that residence time is essential to polymerize hydrochar from a soluble substance at a specific temperature, and together with temperature, governs the geometric characteristics of hydrochar.

To understand the effect of temperature and residence time, researchers use hydrothermal severity to evaluate the degradation and conversion of biomass, and the hydrothermal process is generally regarded as a method to pretreat the lignocellulosic biomass for subsequent enzymatic processes, nutrient recovery, and/or other utilizations [65]. Hydrothermal severity (R_0) is a function of the combined effect of processing temperature and residence time, based on the equation [65,66]:

$$R_0 = t \times \exp[(T - 100)/14.75]. \quad (1)$$

Some studies used a combined severity factor:

$$R = \log(R_0) - pH \quad (2)$$

In previous research, typical lignocellulosic biomass was treated with different hydrothermal severities, and the corresponding solid hydrochar yields are summarized in Table 2. High hydrothermal severity generally generated a low hydrochar yield because of the hydrolysis and degradation of the hemicellulose and cellulose in biomass. The conversion processes of the corresponding components will be discussed in Section 3. Thus, the specific hydrothermal severity should be controlled when hydrochar is to be used for further enzymatic hydrolysis and the liquid product is used to recover nutrients such as xylose and glucose, because degradation or inhibitor formation can occur [67].

2.2.3. Feedwater pH

Studies have observed a decrease in pH for the production of organic acids during the HTC process. Organic acids serve as critical intermediate during the reaction series to catalyze the decomposition of biomacromolecules and hydrochar formation. Hence, variations in the pH during the hydrothermal process can have a marked influence on the characteristics of hydrochar. Generally, the HTC process is considered to be autocatalytic for the formation of organic acids such as formic, acetic, lactic, and levulinic acid from biomass, resulting in a decrease in pH [24,29]. However, the addition of acids or alkali can be used as a catalyst during processing, leading to an increase in proton or hydroxide ion concentration that results in elevated ionic strength, accelerating the reaction rate or tailoring the reaction pathway to achieve the desired hydrochar [17,29,49]. Acids and bases have been utilized in HTC experiments for different objectives. For example, the addition of NaOH, KOH, or $Ca(OH)_2$ as catalysts to facilitate the production of hydrogen-rich gas [72,73]. Extremely acidic or basic hydrothermal conditions can lead to significantly different results by changing the process water, which determines the favored reaction pathway. Lu et al. [74] compared the effects of cellulose HTC in the presence of different initial concentrations of acidic and basic conditions using HCl, H_2SO_4, NaOH, and $Ca(OH)_2$; results indicated that all additives accelerated the dissolution of the solid cellulose, and accelerated the conversion of glucose as concentrations increased. Furthermore, data indicated that the presence of acids enhanced dehydration, which remained a predominant carbonization mechanism resulting in significantly decreased oxygen content in the hydrochar. The result also showed that the production of CO_2 by the acid additive enhanced decarboxylation of the decomposition of organic acids [74]. Basic conditions had a similar effect to the presence of acid on solid recovery; however, this environment appeared to significantly influence the decomposition pathway of 5-hydroxymethyl-furfural-1-aldehyde (HMF), which was converted into levulinic or formic acid. Despite this, the addition of a base showed no effect on the dominant dehydration mechanism [74]. A similar result was found by Reza et al. [75]; who determined that HMF had its minimum content at a pH of 12 and 200 °C, but was not detected at 260 °C during fast degradation. Reza et al. [75] performed the HTC of wheat straw at a feedwater pH (2 – 12) prepared by acetic and potassium hydroxide. Results indicated that both hydrochar and liquid products varied with the pH. Low pH conditions lead to less sugars and more furfural derivatives, surface area, pore volume, and organic acids. Lignin was found to be more reactive as compared to hemicellulose and cellulose in basic water. High pH favors the decomposition of lignin; consistent with the high pH value of water

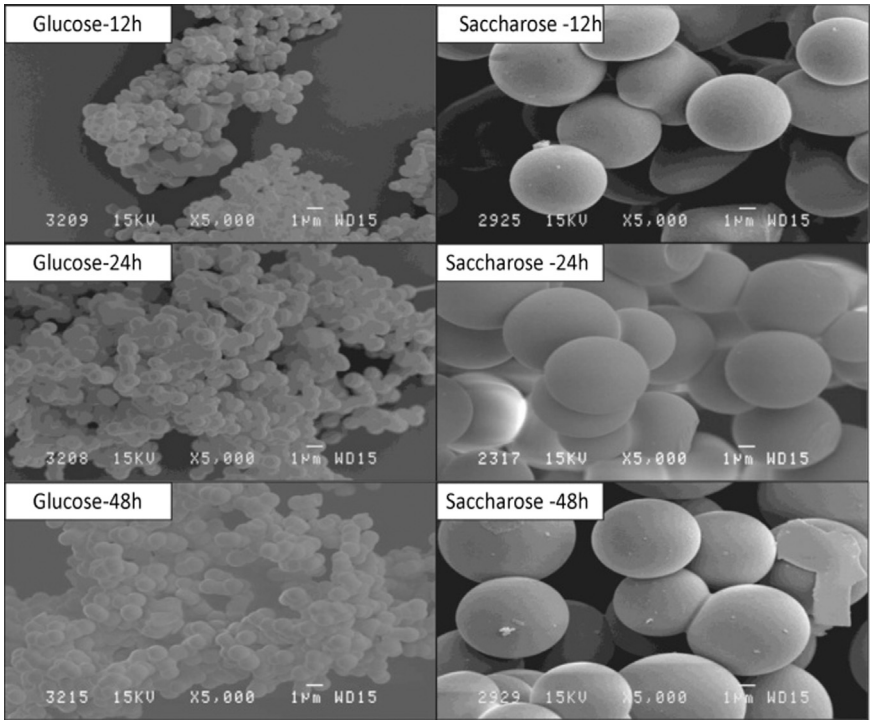

Fig. 3. Hydrochar derived from glucose and saccharose with different residence times from 12 h to 48 h [63].

Table 2
Hydrothermal severity and the corresponding hydrochar yield from lignocellulosic biomass.

Biomass	Temperature (°C)	Residence time (min)	Severity ($logR_0$)	Hydrochar yield (%)	References
Corn stover	170	3	2.538	87.7 ± 0.6	[65]
	210	10	4.239	63.0 ± 0.4	
Poplar	170	15	3.33	76.5	[68]
	200	15	4.12	60.0	
Pine sawdust	170	15	3.33	81.0	[68]
	220	15	4.69	66.0	
Oil palm empty fruit bunch	150	60	3.3	85.4	[69]
	150	240	3.9	81.9	
	190	20	4.0	72.2	
Oil palm frond fiber	210	20	4.54	67.8	[70]
	250	20	5.72	52.7	
Rapeseed straw	170	10	3.33	70.08	[71]
	190	30	4.19	57.47	
	230	10	5.10	51.25	

during hydrothermal processes for the purpose of hydrothermal liquefaction. Phenolic substances such as catechol and guaiacol were observed, and their concentrations increased slightly in basic water; indicating the decomposition of lignin to monomers [75]. Based on these results, it is not surprising that the catalytic role of high pH in HTC leads a lower solid yield by accelerating the processes of hydrolysis or decomposition during hydrothermal liquefaction. Yang [76] investigated the HTC of husks and nuts at a range of pH (4–13). Results indicated that a high pH (13) significantly reduced the solid yield while there was no marked change when pH ranged from 4 to 10. The low solid yield at high pH was mainly attributed to the decomposition of lignin, which showed a limited link with temperatures from 180° to 260°C. Although a high pH was used in the hydrothermal process, the final pH tended to be neutral or acidic; further demonstrating acid production during the HTC. The work of Flora et al. [77] showed that the final pH of the filtrate was significantly different but varied within a narrow range (4.98–5.21) during the HTC of foodwaste using HCl and NaOH additives.

These findings highlight the strong influence of acid and basic additives to the processing water, and how the hydrochar composition, coupled with process mechanisms, can be determined by the hydrothermal environment. In particular, the addition of acid accelerated hydrolysis and decomposition by enhancing the intermediate products, including organic acid production and decarboxylation for CO_2 production. In addition to changing the hydrothermal processes, pH variation also impacts the physical features of hydrochar. For example, lower pH feedwater was critical to the pore structure for the acceleration of the hydrolysis of carbohydrate and enhanced microsphere formation in the early stage of the reaction [78]. A higher adsorptive capacity was generally observed for hydrochar processed with HCl as compared to hydrochar processed with deionized water and NaOH due to differences in ionic strength [77]. In a study by Reza et al. [75], the hydrochar produced from pH 2 feedwater had 2.7 times more surface area as compared to that produced at a pH of 12. The acid feedwater lead to hydrochar with a greater surface area, pore volume, and lower pore size. However, NaOH and HCl additives to sludge during subcritical conditions showed a statistically insignificant influence on the mean moisture diffusivity of hydrochar. The mean moisture diffusivity of hydrochar produced using H_2O was higher as compared to hydrochar produced with NaOH and HCl [79].

2.2.4. Substrate concentration

High concentrations of substrate employed in the HTC reaction are likely to achieve high productivity levels; however, few studies have focused on the effects of concentration on the HTC process. Knezevic et al. [80] demonstrated that a high initial concentration of glucose produced HMF that rapidly produced a polymerization reaction. Although increased concentrations of raw substrate have shown inverse relationships for liquefaction reactions during the HTC process, the products obtained from raw biomass may partly produce polymerization due to the incomplete hydrolysis of polymers. Insoluble matter could be explained by a pyrolysis-like process, which performs at

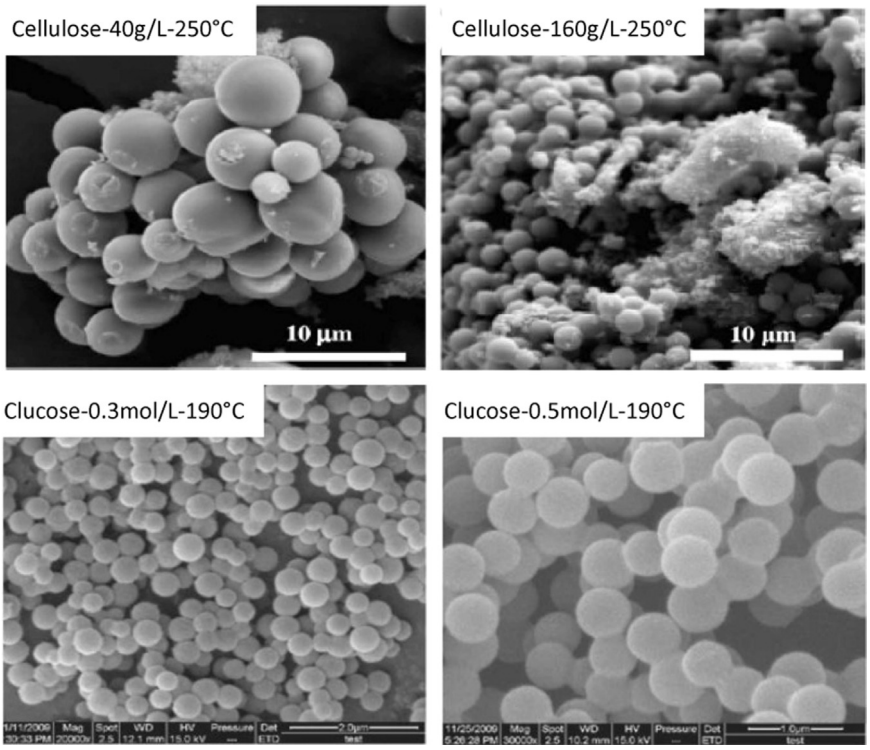

Fig. 4. Hydrochar derived from cellulose and glucose with different concentration [53,81].

relatively higher outer pressures with limited water under subcritical conditions. Conversely, raw biomass required more heat energy and a long residence time to break down polymers and generate enough monomers to reach solution equilibrium and finally precipitate solids [17]. Sevilla et al. [53] reported that an increased cellulose concentration lead to a decreased yield of hydrochar, and that solid products showed relatively high O/C and H/C. Their results showed that the incomplete hydrolysis process lead to the formation of some monomers, which produced precursors for polymerization or condensation. As such, a longer residence time may be required for the HTC of raw biomass as compared to the pure chemicals in models. At the same time, due to the insufficient polymerization reaction of soluble products derived from high concentrations of raw biomass, solid products may have a lower degree of microsphere agglomerates, which can be inferred from the microsphere diameter. For example, in research by Sevilla [53], the increased concentrations of cellulose (from 40 to 160 g L^{-1} at 250 °C) resulted in the formation of smaller microspheres. As shown in Fig. 4, when the direct utilization of the dissolved substrate or easily dissolved substrate such as glucose and sucrose occurred, results showed a reversed trend; the size of the hydrochar particles increased at high substrate concentrations [56,63,81]. The high concentrations of dissolved substrate may directly enhance the rapid polymerization of soluble substances that agglomerates microspheres to form bigger spherical particles. Hence, we can conclude that the properties of hydrochar derived from varied concentrations depends heavily on the nature of the precursors and the hydrothermal conditions; in particular a residence time which provides sufficient time for the production of soluble products and polymerization. Systematic studies are needed to investigate the variation of concentrations of biomass and single components on the properties of hydrochar.

2.2.5. Heating rate

Heating rate is another factor impacting the HTC process. Generally, a higher heating rate does not favor hydrochar formation. Zhang et al. [82] studied the influence of heating rates (5–140 °C min^{-1}) on the hydrothermal process of grassland perennials and results suggested that hydrochar yield decreased from 22% to 23% to 8–9% when the heating rate increased. In another study, Zhang et al. [83] determined that the yield of hydrochar decreased from approximately 19–9% as the heating rate increased from 5° to 140°C min^{-1} when the hydrothermal process used corn stover and wood chips as feedstock. After the dissolution and stabilization of the fragmented compounds in the hydrothermal process, secondary reactions occurred for the bulk fragmentation of biomass and decreasing the heating rate could result into more solid residue formation [4]. Heat and mass transfer limitations can be reduced using a high heating rate and the time available for the secondary reactions of the intermediate products during HTC is also minimized [84]. Hence, a high heating rate is generally used for the hydrothermal liquefaction process. A similar tendency was found in a study by Brand [85], which investigated the effect of heating rate on the hydrothermal conversion of pine sawdust and cellulose; results indicated that increasing the heating rate from 2° to 20°C min^{-1} was beneficial for biomass conversion into bio-oil, indicating that a decreased tendency was observed for hydrochar formation. Furthermore, at low heating rates, the O/C and H/C ratios decreased as the temperature and residence time increased. Thus, a low heating rate may enhance the degree of carbonization in hydrochar, which explains the relatively low HHV of hydrochar obtained at high heating rates, and indicates that an appropriate heating rate can be selected during HTC to control the distribution of the hydrochar and liquid products. The relevant properties of hydrochar in relation to heating rate are summarized in Table 3.

3. The formation mechanisms of hydrochar: N-free biomass and N-rich biomass

3.1. N-free biomass for hydrochar formation

3.1.1. Cellulose to hydrochar

Generally, cellulose is the largest part of lignocellulosic material, consisting of D-glucose subunits, linked by β − 1,4 glycosidic bonds [86]. The cellulose in lignocellulosic materials consists of crystalline

Table 3
Effects of the different process parameters of HTC on the physical/chemical characterization of hydrochar.

Increase parameters	Solid yield	BET surface area	Porosity	H/C	O/C	Energy densification	Equilibrium moisture
Temperature	−	+	+	−	−	+	−
Residence time	−	+	+	−	−	+	−
Feedwater pH	ND	−	−	+	+	ND	ND
Substrate concentration	ND	ND	ND	+	+	ND	ND
Heating rate	−	ND	ND	+	+	−	ND

"+": increase effect. "–": decrease effect. ND: not determined.

fibers, and parts with a disorganized, amorphous structure; these cellulose chains mostly assemble into independent cellulose fibers which are weakly joined through hydrogen bonding [87].

The disruption of cellulose in the hydrothermal process is performed at a relatively high temperature above approximately 200 °C. The physical structure of cellulose is initially disintegrated by hydrolysis. Long chain cellulose breaks down to smaller molecular weight water soluble compounds (oligomers) and then further to glucose (monomers), which partly isomerizes to fructose [53,88]. The hydrolysis products subsequently undergo a series of isomerization, dehydration, and fragmentation (ring opening and C–C bond breaking); producing key intermediates 5-HMF or furfural and their derived products. These intermediates undergo further polymerization and condensation reactions combined with reverse aldol condensation and intermolecular dehydration [17,89].

The intermediates in the decomposition process also produce organic acids including acetic, lactic, propenoic, levulinic, and formic acids which lower the pH of the reaction medium, and the acidic conditions favor the further degradation of the intermediates; for example, the dehydration of glucose into HMF [17,58,90]. Organic acids (e.g., acetic acid) catalyze the reaction process and can be used to obtain a different distribution of the objective product [75]. During the transformation from polymers to hydrochar, intramolecular dehydration and keto-ento-enol tautomerism are thought to occur due to the increasing production of double bonds, which is favored by aromatization. Thus, aromatization reactions increase the concentration of aromatic clusters in the aqueous solution which ultimately reaches the critical supersaturation point under such conditions, leading to burst nucleation [53]. The nuclei formed grow outwards by diffusion and linkage of the chemical species presented in the solution to the nuclei surface; and this linkage forms reactive oxygen functional groups such as ether and quinine [53]. When the growth stops, the outer surface of the hydrochar particles will contain a higher concentration of reactive oxygen species as compared to the core [53]. This model of hydrochar particles, with a hydrophobic core and hydrophilic shell, was proposed by Sevilla et al. [53,56]. Moreover, Gao et al. [36] used a scanning electron microscope (SEM), transmission electron microscopy, fourier transform infrared spectroscopy (FTIR), and X-ray photoelectron spectroscopy (XPS) to analyze the hydrochar derived from cellulose at a HTC of 250 °C, and showed a core-shell structure of the hydrochar. The core contained ketone and ether groups while the shell contained carboxylic and carbonyl groups. Based on these findings, the mechanism for transforming cellulose to hydrochar is summarized in Fig. 5. Detailed information on the formation mechanisms of hydrochar can be found in previous studies [53,56,90].

Considerable research has focused on determining the structural characteristics of hydrochar, to better to understand its formation processes and those of other materials including starch, hemicellulose, sucrose, and fructose. For example, Sevilla et al. [56] identified a core-shell structure exhibiting a highly hydrophobic aromatic nucleus with a hydrophilic shell consisting of high concentrations of reactive oxygen functional groups such as hydroxyl/phenolic, carbonyl, or carboxylic using FTIR, Raman, and XPS techniques on hydrochar from glucose performed at 170–240 °C. Their research highlights the presence of an aromatic nucleus with stable oxygen forming groups in the hydrochar structure [56]. In another study, a similar structure was found in hydrochar derived from cellulose produced at temperatures in the range of 220–250 °C; it was inferred that the solid product consisted of small clusters of condensed benzene rings which was also considered to be the carbonaceous scaffold [53]. However, in Titirici et al. [91], advanced solid state ^{13}C nuclear magnetic resonance (NMR) experiments were performed with the hydrochar using glucose and the intermediate product HMF as carbon sources at 180 °C for 24 h. Results showed that the local structure condensed to hydrochar with a structural composition similar to HMF [91]. Separate research proposed that, "the core of the carbonaceous material is mainly composed of cross-linked furanic by domains containing short keto-aliphatic chains," which highlighted a furanic structure as opposed to benzene rings [92]. These two structural models suggest entirely different structural compositions for hydrochar. However, Chuntanapum et al. [93], proposed a structure with some furan units coupled with benzene rings. The hydrochar (called tarry material in the work), derived from 5-HMF when hydrothermal temperatures were set at 350 °C and 450 °C and analyzed using FTIR and Raman spectroscopies, indicated the presence of the 5-HMF functional groups and the existence of benzene rings in the char structure [93]. These differences may be attributed to the vastly different hydrothermal conditions in these experiments, especially with respect to temperature and residence time.

Later, Falco et al. [94] estimated the furanic-to-arene ratio by comparing the ^{13}C NMR spectra of char obtained from glucose at 180 °C with a 12 h residence time with the process of pyrolysis. They found that it was possible to change the furanic-to-arene ratio in the aromatic core of the hydrochars; however, this was not possible when the calcination process was used alone [94]. In another paper, Falco et al. [64] proposed the model for cellulose HTC under mild temperatures (180–280 °C), and the study also confirmed that a final hydrochar comprised of extensive aromatic networks or a polyfuranic structure formed through two possible mechanisms, which were interchangeable based on the temperature. These studies highlight the major routes for the formation of hydrochar derived from cellulose.

In conclusion, the cellulose derived hydrochar exhibits a polyaromatic structure combined with polyfuranic rings; the presence of which depends on the hydrothermal severity, especially high temperatures and long residence time. The mechanisms of hydrochar formation from cellulose are shown in Fig. 5.

3.1.2. *Hemicellulose to hydrochar*

Hemicellulose is a complex polymer of pentose such as xylose and hexose sugars other than glucose, which has a lower degree of polymerization as compared to cellulose [86]. It is found in lignocellulose materials, associates cellulose with hydrogen bonds, and forms covalent bonds with lignin, enhancing the rigidity of plant cell walls [95]. At certain temperatures, hemicellulose is easy to separate from the main ingredients and is more likely to collapse into monomers. Generally, hemicellulose consists of various sugars (mainly xylan and glucomannan) which contain short lateral chains, acetic acid, pentoses, (β-D-glucose, β-D-mannose, α- D-galactose), hexuronic acids (β-D-glucuronic acid, α-D-4-O-methylglucuronic acid, α-D-galacturonic acid), and deoxyhexoses (α-L-rhamnose, α-L-fructose), which make them more susceptible to chemical degradation [89].

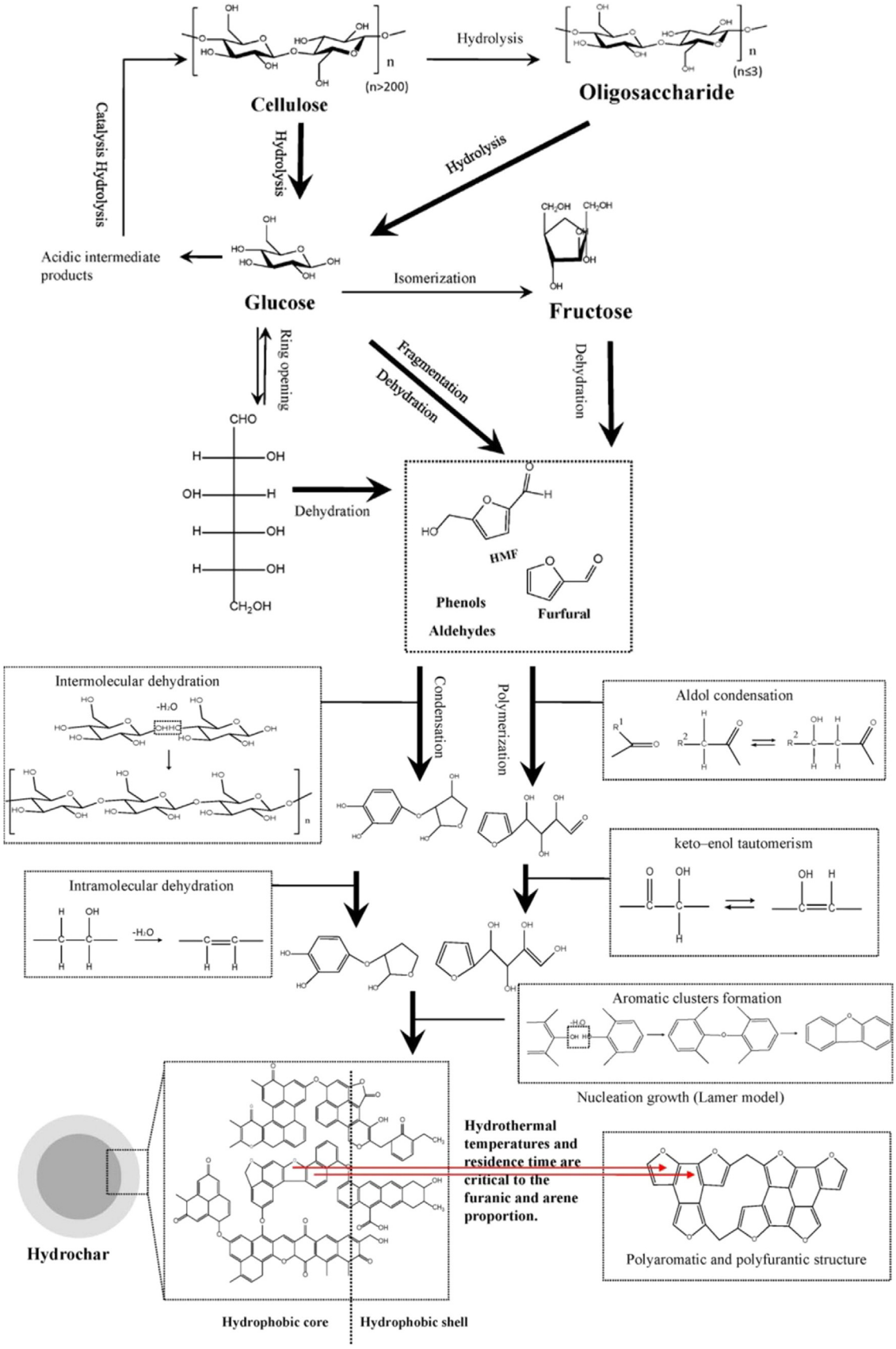

Fig. 5. Hydrochar formation mechanism from cellulose [53,56,94].

The two dominant categories of hemicelluloses described above are thermally unstable. Similar to cellulose, hemicellulose polymers dissolve at approximately 180 °C during the hydrothermal process [50,86]. When temperatures increase above 180 °C, the derived monomers go through an exothermal reaction which leads to the consecutive reaction mentioned above [86]. Research has focused on the discussion of xylose as the major species depolymerized from the xylan of hemicelluloses. Qi et al. [96] investigated the non-catalyzed decomposition of D-xylose (180–220 °C), and found that the main products were furfural and formic acid derived from the further degradation of furfural under the same conditions. Paksung et al. [97] also found that furfural and retro-aldol condensation products were the major liquid intermediates in subcritical water. Retro-aldol condensation products accounted for the largest proportion in subcritical water, while furfural was dominant in the supercritical region. With increasing temperatures and reaction times, the color of reaction residue became darker and the organic carbon in liquid was not balanced because the decomposition product, furfural, polymerized to dark, insoluble substances [96]. Titirici et al. [91] compared hydrothermal carbons derived from monomers, xylose, and furfural using SEM, ^{13}C solid-state NMR, and elemental analysis; they demonstrated that furfural dehydrated from xylose and the pure furfural could produce very similar carbon materials. These were well dispersed, separated spherical particles arbitrarily called carbon-β. Hence, the furfural, an important intermediate dehydrated from xylose, will sequentially undergo polymerization reactions to form hydrochar [61]. The formation pathways of D-Xylose derived hydrochar are shown in Fig. 6.

3.1.3. Lignin to hydrochar

Lignin is an amorphous heteropolymer composed of three methoxy-substituted phenyl propane units (p-coumaryl, coniferyl, and sinapyl alcohol), which is extensively cross-linked to establish a steady skeleton for plant cell walls. Furthermore, except for physical admixtures, lignin is generally associated with hemicelluloses through covalent bonds; making mechanical destruction and microbial attack difficult [86].

Similar to hemicellulose, lignin starts to dissolve at temperatures of 200 °C; however, relatively low amounts of lignin dissolve in the water. The behaviors of lignin under subcritical water and supercritical water depend heavily on the precursor and process conditions. Due to its random structure and high molecular weight polymers, the reaction mechanisms of lignin are complex. Studies have used isolated lignin monomers, such as catechol [98], guaiacol [99], eugenol [100], and other phenolic model compounds like vanillin [101] and diphenylether (DPE) [102] to explore lignin reaction pathways, with various conclusions. However, HTC is generally performed in the subcritical water region (> 300 °C), which differs from supercritical water conditions where lignin undergoes a water soluble and totally homogeneous reaction, because the lignin only partly hydrolyzes. The degradation of lignin in the HTC process is similar to pyrolysis; however, due to the presence of subcritical water, the soluble fraction reactions are different. The temperature of the solvent is also a critical factor in lignin depolymerization because high temperatures lead to an increase in water density which can facilitate the repolymerization of monomers [103]. The reaction time is also critical since the formed monomers, such as the guaiacol reaction with higher molecular weight compounds, form phenolic char [104].

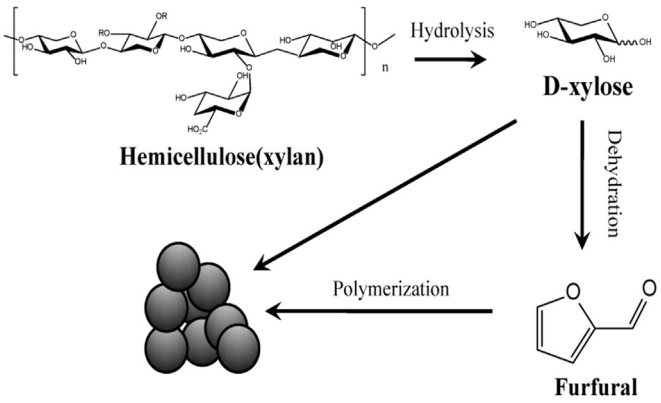

Fig. 6. Brief formation pathways of hemicellulose (D-Xylose) to hydrochar [61].

A simplified mechanism of the degradation of poplar lignin based on two-phase hydrothermal reactions was proposed by Bobleter et al. [105]. Firstly, lignin underwent a rapid fast reaction phase and degraded into the soluble fragments, then a slower reaction phase, where repolymerization occurred through the reaction of soluble fragments with one another. Zhang et al. [106] conducted research into the hydrothermal treatment of Kraft pine lignin and their results followed the two-phase mechanism mentioned above. As the temperatures increased, the Kraft lignin became more water soluble within a very short period; then, there was a slow reaction phase, in which the soluble fragments interacted and recondensed into solid residue. On this basis, Fang et al. [104] summarized previous research and proposed a scheme for the different reaction pathways towards the dissolved products and non-dissolved lignin in homogeneous and heterogeneous environments. Solid residue formed in two main ways. Firstly, the dissolved lignin decomposed by hydrolysis and dealkylation in a homogeneous reaction which yielded phenolic products such as syringols, guaiacols, catechols, and phenols; these intermediates undergo a cross-linking reaction and are re-polymered into phenolic char; Alternatively, the non-dissolved lignin, not completely solved at low temperatures, underwent solid–solid formation mechanisms similar to pyrolysis, which yielded highly condensed char with polyaromatics in the heterogeneous environment [104]. However, reactions during the HTC process may favor solid–solid formation due to the low production of soluble intermediates which results in low phenolic char. As hydrothermal severity increases, the solid–solid conversion may enhance polyaromatic char production. The simple formation mechanism of lignin derived hydrochar is illustrated in Fig. 7.

3.1.4. Lignocellulosic biomass to hydrochar

Lignocellulosic biomass, produced by terrestrial plants, represents a non-food, sustainable resource predominantly composed of polymers, cellulose, hemicellulose, and lignin combined with low molecular weight substances including inorganics and extractives [86]. Fig. 8 shows the basic structure of lignocellulosic biomass. The hydrochar formation mechanism for the main components of lignocelluloses has been summarized in the previous sections. However, these sections discussed the reaction mechanisms of pure substances. In fact, lignocellulose is highly complex, and its composition influences the various reaction pathways. Nevertheless, because the three main constituents of lignocellulose act as precursors for the hydrochar product, it is essential to elucidate interactions during the decomposition process and the mechanisms involved in solid formation.

Recently, considerable research and industrial applications have focused on lignocellulose pretreatment techniques, such as chemical treatment [107], biological treatment [108], and thermal treatment or a combination thereof [109,110] to obtain more easily processed materials which can be further transformed into different chemicals with different purposes. For example, the recovery of reducing sugar and ethanol fermented from (hemi-) cellulose and methane production by anaerobic digestion. It can be concluded the primary purpose of these applications is to destroy the structure of the biomass by altering or breaking the lignin seal and disrupting the crystalline structure of cellulose [111]. The HTC of lignocelluloses follows the same approach by breaking up the structure for more favorable degradation. The hydrolysis process is crucial to damage the structure of lignocellulose components and to reduce the degree of polymerization of the biomass. The lignin serves as a template for the orientations of polysaccharides because it is necessary to break the covalent bonding between lignin and

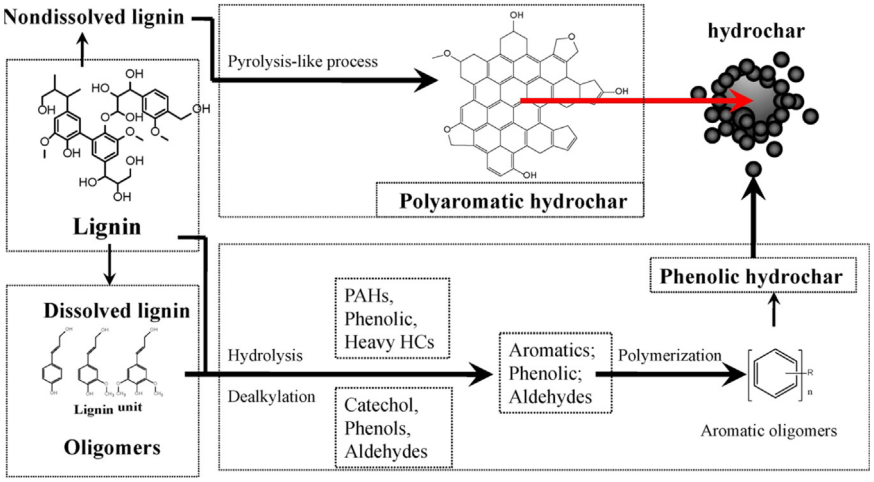

Fig. 7. Simple formation mechanism of lignin derived hydrochar during HTC according Fang et al. [104] and Kang et al. [61]: the two reaction pathways via liquid state and solid state to form hydrochar and the phenolic hydrochar may present on the surface of polyaromatic char derived from the non-dissolved fraction of lignin.

xylans or cellulose and the internal hydrogen bond in cellulose for further degradation [112].

The fracture of the raw biomass is different to the decomposition of single components due to the strong connections between components, including covalent bonds and hydrogen bonds. Falco et al. [64] reported that the temperature during the formation of hydrochar derived from rye straw started at, and shifted to higher values as compared to pure cellulose. Thus, fully carbonized materials can be achieved from the pure feedstock. This also confirms that the raw lignocellulose requires a higher activation energy to disrupt the structure of the individual components. Hence, the hydrochar production not only depends on the composition of the lignocellulose, but is also determined by the hydrothermal conditions. Generally, the component degradation level for lignocellulose follows the order lignin < cellulose < hemicellulose at the same hydrothermal severity. The phenolic structure of lignin was the main reason for the stability, and its benefits for the condensation reaction [61]. As compared to cellulose which has a partly crystalline structure, hemicellulose has a lower molecular weight with a lower degree of polymerization (approximately 50–200), and its amorphous properties mean that it is more easily vulnerable to attack in the critical hydrothermal environment [113].

Lu et al. [37] compared the hydrochars from feedstock with a single chemical composition with those from mixed feedstock, and their results showed that complex feedstocks needed a longer residence time to reach stable solid recovery due to the interaction between components. Lignin content has a marked effect on carbohydrates in the biomass because it serves as a plant wall support; stabilizing the cellulose by preventing disruption in the crystalline structure at low temperatures. Furthermore, by enclosing cellulose and hemicellulose, lignin slows down the release of monosaccharide, which would further hinder the formation of intermediate products. Li et al. [114] reported that lignin migrated out of the poplar wood cell wall and was finally deposited on the cellulose surface during HTC. This negative influence was attributed to the insoluble lignin content which retarded hydrolysis [115]. The surface blockage of cellulose by lignin may inhibit further degradation. We can conclude that HTC has negligible effects on lignin; however, its presence has a marked effect on the degradation of lignocellulosic biomass during the hydrochar formation. Lignin also contributed to the perseverance of the natural macrostructure of the initial lignocellulosic biomass in the hydrochar [64]. For example, Herbert et al. [116] reported that a high lignin content resulted in the initial structure of the raw lignocellulose being retained in the solid product, with only soluble constituents being converted.

It is apparent that the carbonization process can assume two pathways; the dissolution of intermediate products through polymerization, and pyrolysis-like decomposition relying on hydrothermal severity.

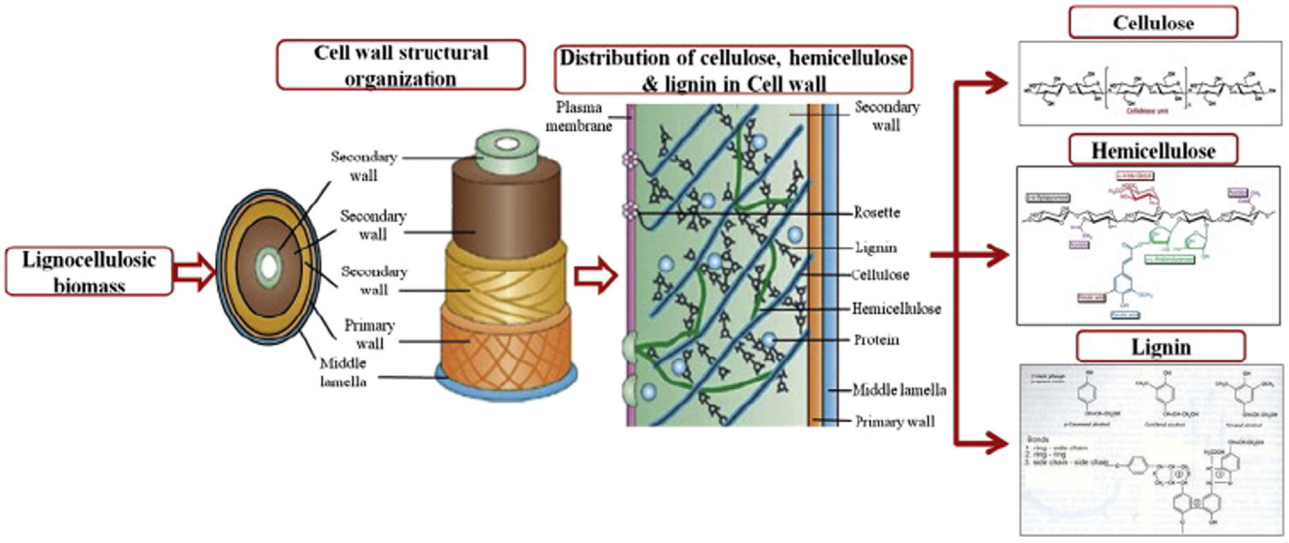

Fig. 8. The diagrammatic illustration of the framework of lignocelluloses [5].

Because the hemicellulose in biomass can hydrolyze at a lower temperature, polymerization mainly happens in the homogenous reaction. The first approach includes the dissolved part of the cellulose and lignin because the amorphous cellulose is easily collapsed under subcritical conditions. However, the second pathway may undergo a pyrolysis-like process for the undissolved biomass. The crystalline regions of cellulose and lignin need to be treated at high intensity; hence, when the hydrothermal conditions do not provide the activation energy, the individual components do not release from the body of the biomass and a pyrolysis-like process will occur. Differing from pyrolysis, this process is performed in a different medium with higher pressure in the homogeneous phase. The products of the pyrolysis-like process have a relatively higher aromatic structure from the lignin, which shows limited modification. The whole process can form two types of carbon: the char formed from condensation including, phenolic char and polyraromatic with polyfuranic char; and the char derived from the pyrolysis-like process producing lignin and cellulose pyrolysis-like char. However, in a homogeneous process, these various carbons may go through automatic integration such as molecule rearrangement and dehydration, and unified hydrothermal carbonization products are formed when high temperatures or residence time was used. The formation mechanisms for biomass derived hydrochar are illustrated Fig. 9.

3.2. N-rich biomass to hydrochar formation

3.2.1. Protein and amino acid conversion

Sewage sludge (SS) represents a major solid waste derived from municipal waste water treatment plants. The increasing quantities of SS and their disposal present many environmental concerns and health hazards [118]. However, SS is a complex waste that is rich in organic substances and nutrients (such as N and P); composed of microorganism constituents (nucleic acids, proteins, carbohydrates, and lipids) and their decay products; undigested organic material; and inorganic material such as salts and heavy metals which make SS difficult to deal with [119]. Microorganisms, especially bacteria, contained in SS are critical active agents for wastewater treatment; they break down the organic fraction in SS and store the nutrients. Hence, carbohydrates and proteins comprise the main organic components in SS, with lignin accounting for a small component which can produce high value biopolymers [60].

Compared to lignocellulosic materials, the HTC decomposition of organics contained in the SS is more complex. The carbohydrate fraction may experience a similar pathway as lignocellulose for the hydrolysis of oligosaccharides to monosaccharides, which would undergo further reactions to form hydrochar. Due to a large component of protein being derived from bacteria, the reaction pathways of SS are markedly different. Consequently, it is essential to explore the behavior of proteins in the hydrothermal environment.

The proteins in the hot pressed water would firstly hydrolyze into amino acids by breaking the peptide bond, which is a C–N bond between the carboxyl and amine groups, present in all amino acids [120]. This depolymerization process is slower than carbohydrate hydrolysis due to the peptide bond in the protein being more stable than the $\beta-1,4$- and $\beta-1,6$-glycosidic linkages in cellulose and starch; however, it can be rapidly catalyzed in an alkaline or acidic reaction medium, especially in the acidic environment produced from the degradation of saccharides [121,122]. Furthermore, several amino acids including leucine, isoleucine, phenylalanine, serine, threonine, and histidine have been found to be unstable at acidic and near-neutral pH [122]. Moreover, the decomposition depended heavily on the type of amino acid, the hydrothermal condition employed, and the solution pH.

Various amino acids have been employed as model compounds by researchers under hydrothermal conditions. For example, decarboxylation and deamination were the major reactions of amino acids observed at relatively short residence times in the studies using glycine and alanine as model compounds [123,124]. Moreover, the decomposition of the mixed amino acid can be influenced by each other, and ammonia, amines, CO_2, and organic acids were the main decomposed products [122,124]. The deamination of amino acids produced ammonia, which survived in the liquid as ammonium ions, representing a component of inorganic nitrogen which can lead to a reduction of organic nitrogen from the raw feedstock.

3.2.2. Sewage sludge to hydrochar

The presence of carbohydrate in SS, especially saccharides, leads to different reaction ways for the pure protein or amino acid. On one

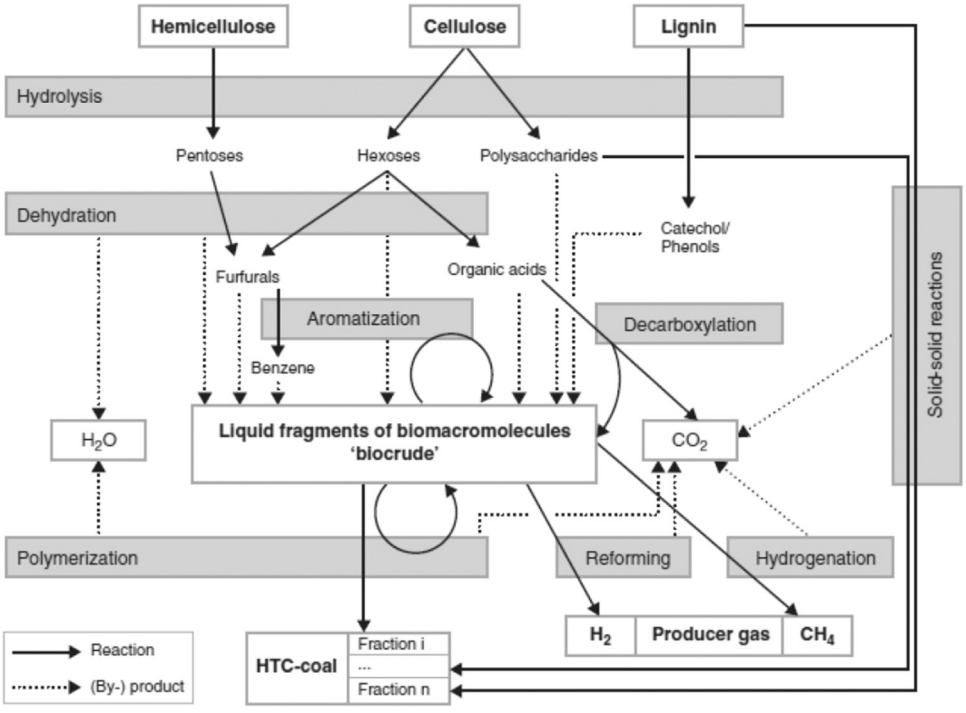

Fig. 9. Process of hydrochar formation mechanisms from lignocelluloses [117].

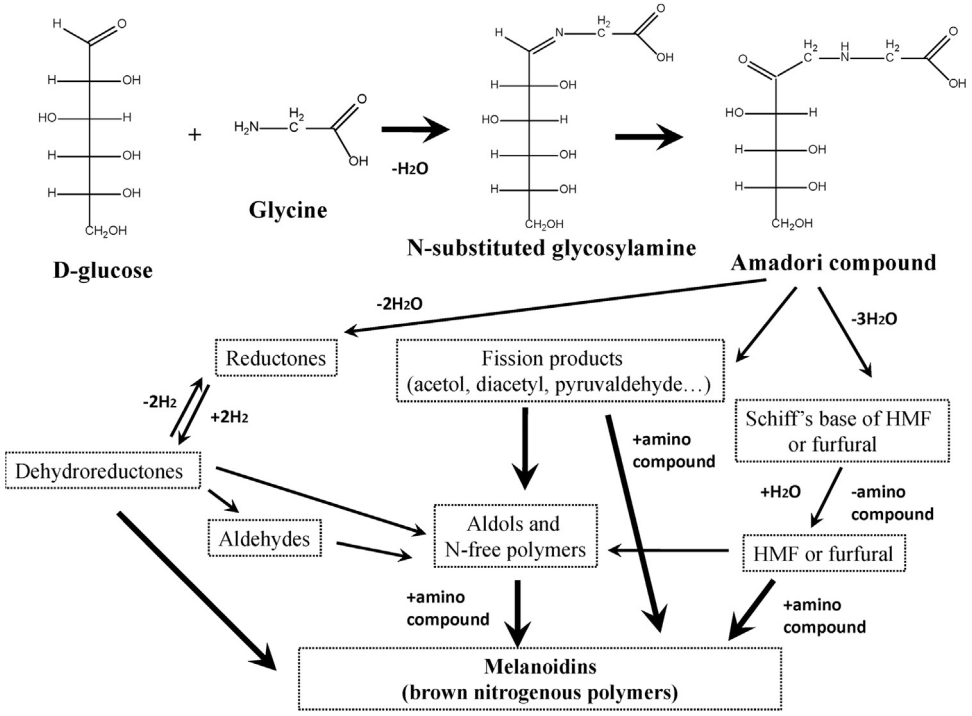

Fig. 10. The typical Maillard reaction between D-glucose and glycine [127].

hand, a relatively low pH for the hydrothermal environment was provided by the conversion of saccharides, which influenced the extent of the amino acid degradation somewhat. Furthermore, several kinds of amino acids, including leucine, isoleucine, phenylalanine, serine, threonine, and histidine have been found to be unstable at acidic and near-neutral pH [122]. E. Danso-Boateng et al. [125] found that the organic compounds, such as acetic acid, benzene, acetic acid, butanoic acid, pentanoic acid, and propanoic acid in the HTC liquid of primary SS provided catalytic conditions for the degradation of SS. Hence, the hydrothermal feed water had a marked influence on the degradation behavior of the protein and derived amino acids.

On the other hand, with a long residence time, the amino acids derived from SS initially undergo the Maillard reaction with sugars or the degradation products of sugars which contain carbonyl groups to produce N-containing ring compounds. The Maillard reaction occurs between the amine group of the amino acid and carbonyl group of a sugar, and polymeric compounds which could be called melanoidins are formed [126]. The typical Maillard reaction between D-glucose and glycine is shown in Fig. 10 [127]. This reaction explains the interactions between proteins or amino acids and sugars in SS resulting in the formation of brown hydrochars with a characteristic odor. He et al. [60] reported that the HTC of SS produced uniform brown hydrochars with a nut-like smell that exhibited strong evidence of a Maillard reaction. E. Danso-Boateng et al. [125] identified several Maillard products including aldehydes, furans, pyrroles, pyrazines, and pyridines in liquid samples derived from the HTC of primary sewage sludge at 180 °C and 200 °C, and reaction times between 30 and 240 min. Their results also showed that there were no Maillard reaction products when the primary sewage sludge was carbonized at 140 °C for 240 min and at 160 °C for 60–120 min; however, the Maillard reactions dominated when HTC was conducted at temperatures starting at 180 °C for reaction times longer than 15 min. Therefore, we can conclude that hydrochar formation may depend on the composition of the SS, protein species, and amino acids as well as the hydrothermal temperature.

It is important to achieve hydrochars with lower N content when they are used as solid fuel, and to improve the content of total N and organic N in the aqueous phase for the recovery of N in amino acids or ammonium salts. Seiichi Inoue et al. [128] examined the nitrogen in SS and found that solubilization and decomposition started above 150 °C and the N was transformed into the aqueous phase. He et al. [129] found that the increase in hydrothermal temperatures led to large conversions of initial protein into ammonium in liquid, and had a marked influence on the N distribution. Hence, maintaining a suitable residence time and temperature is necessary to the distribution and mass balance of N. The detailed N conversion, distribution, and its role during HTC will be discussed in the following chapter.

Based on the pathways from carbohydrate, coupled with the degradation of protein during the HTC process, SS hydrochar formation pathways follow two approaches. First, the dissolved fractions of carbohyrates and proteins undergo a series of hydrolysis, dehydration, and Maillard reactions contributing to the formation of polyaromatic hydrochars. The undissolved fraction of SS is thought to undergo a solid–solid conversion, similar to pyrolysis, with condensation, dehydration, and decarboxylation. He et al. [60] proposed a simple schematic of hydrochar formation pathways from SS using HTC, and these mechanisms are shown in Fig. 11.

However, SS had a high content of N relative to carbohydrate or lignocellulose, hence, it is difficult to determine the hydrochar structure due to the high nitrogen source of protein or amino acids. Model compounds were used to understand the formation process employing carbohydrate and amino acids. For example, Baccile et al. [130] studied the hydrochar obtained from glucose and glycine representative model compounds to simulate pure carbohydrates in the presence of natural amino-containing compounds with a hydrothermal reaction at 180 °C for 12 h. Their ^{13}C and ^{15}N NMR results indicated that the initial glycine and glucose completely rearranged into an extended pyrazo-furanic matrix, and the possible molecular structure, aromatic units, pyrazine or pyridine, phenols, and pyrrole type compounds were also proposed. An extended nitrogen-containing aromatic network bounded with a polyfuran network formed, which contrasts with the widely held view that a higher temperature (< 180 °C) could increase the degree of aromatics in the pure carbohydrates. However, the hydrochar obtained in this study already possessed an increased level of aromatics, with several N-containing materials [130]. Based on the N introduction to

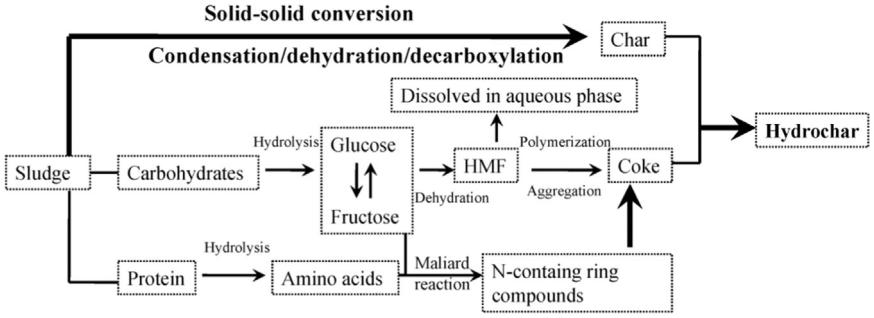

Fig. 11. Schematic hydrochar formation mechanism from SS [60].

the hydrochar, Sevilla et al. [131] synthesized microalgae-derived hydrochar with a D-glucose additive and their results showed Maillard-type cascade reactions increasing both the C and N content in the hydrochar. The N was incorporated as aromatic heterocycles, such as pyrrolic-, pyridinic-N, and quaternary-N structures. A similar result was also found by Falco [132], who showed that the addition of glucose to the raw algae HTC feedstock enhanced the incorporation of N to the hydrochar as aromatic heterocycles. Hence, the final structure is likely to depend on the raw feedstock (especially the concentration of saccharide due to the generally low saccharide content and high protein content in SS or microalgae) and hydrothermal severity. When the hydrothermal severity was increased, a low N content was achieved; however, N-evolution also occurred. He et al. [129] investigated N-evolution in the SS derived hydrochar, and showed that an increase in temperature led to an increase of pyridine-N. In Falco's study [132], the addition of glucose converted the pyrrolic N into more stable nitrogen groups, namely quaternary and pyridinic-N. However, the N in the hydrochar changed to a more stable form, incorporating into the hydrochar structure.

In conclusion, the N-containing aromatic network was assigned to the main hydrochar structure from the N-rich biomass. However, the chemical processes behind the introduction of N contained in the protein or amino acids and carbohydrate derived hydrochar matrix remains unclear. New technology is needed to establish the specific framework of the hydrochar, and further research should focus on the investigation of complex compounds and the application of N doping material. More information is needed to clarify and detect model compounds and typical biomass (e.g., SS and algae) to a better understand the formation of the hydrochar structure.

4. Characterization of hydrochar

4.1. The proximate and coalification degree

The proximate and ultimate analysis of hydrochar is necessary to ensure the efficient utilization of hydrochar as a fuel. The proximate analysis, including volatile matter (VM), ash, and fixed carbon (FC) content was measured in the products. The elemental composition of the hydrochar, characterized by the H/C and O/C ratios, changed significantly as a result of HTC, and confirmed the carbonization degree of the hydrochar. The mass loss depends heavily on the reaction severity and the composition of the raw materials. Generally, HTC carried out at a high temperature produced a low solid mass yield, however, an increased fraction of fixed carbon in the hydrochar can be achieved, indicating that a significant amount of carbon was retained in the hydrochar. Hydrochar with a high FC and decreased VM content can overcome the drawbacks of raw biomass, which is easily ignited at low temperatures of approximately 250 °C and rapidly reaches maximum weight loss when used as solid fuel [133]. Meanwhile, improved combustion efficiency and reduced pollutant emissions can be expected [134]. Differences in the proximate analysis of hydrochar from different raw biomass derived by the HTC process are summarized in Table 4. As compared to lignocellulosic biomass, SS generally contained lower fixed carbon and higher ash content. With regard to lignocellulosic biomass, the biomass polymers in lignin have a high aromatic structure content. These natural characteristics promote the fundamental formation of hydrochars with high FC.

The H/C and O/C ratios are important criteria for estimating the degree of de-oxygenation, and the aromatic content during the HTC of biomass [135]. They provide clues as to the aromatic content; a higher H/C ratio indicates that the hydrochar aromatic content is lower [135]. Generally, the H/C and O/C atomic ratios are analyzed using a Van Krevelen diagram for the comparison of raw biomass with hydrochar [136]. The H/C and O/C ratios of bituminous coal and lignite were also plotted on the same diagram for coalification comparison purposes [59,137]. As shown in Table 4, the H/C and O/C ratios decreased as the hydrothermal temperature or retention time increased for all hydrochars. The ratio shift can also delineate the reaction pathways; the dehydration (production of H_2O) and decarboxylation (production of CO_2 or carbonyls including carboxylic acids) reaction during the HTC [58]. In Fig. 12, it is apparent that the lignocelluloses derived hydrochar generally showed a high degree of coalification as compared to sludge derived hydrochar, indicating that natural composition plays a significant role during HTC. Berge et al. [42] used mass balance analyses of the distribution of carbon in the gas, liquid, and solid from HTC of MSW, and results indicated that the hydrochar retained a major fraction of carbon structured with high aromaticity, generating lower H/C and O/C ratios. Furthermore, the HTC of food, paper, and mixed MSW were predominantly governed by dehydration, with a slight shift in the O/C ratio for partial decarboxylation reactions [42].

Dehydration can lead to reduction of H/C and O/C ratios simultaneously. The dehydration during hydrothermal carbonization includes both chemical and physical processes, but chemical dehydration dominates the major loss of water from the biomass in the HTC process [17]. However, chemical dehydration occurs more intensely than decarboxylation, and significant decarboxylation may only occur after a certain amount of water is formed in the chemical dehydration process [17]. This chemical loss of water from the biomass in subcritical water conditions can be understood as an assimilating process for dehydration along with the condensation reaction for the production of solid residue. The dehydration mechanism of elimination of hydroxyl groups from the biomass has been widely accepted and decarboxylation was caused by the elimination of carboxyl groups [9,53]. Large weaknesses in O-H stretching vibrations in hydroxyl or carboxyl groups contained in the raw biomass have been verified for the dehydration reaction. However, CO_2 has been shown as the dominant gas product in the decarboxylation process in HTC. Hoekman et al. [58] reported that the gaseous product represented approximately 8% of the starting feedstock mass. The dominant organic acids such as formic, acetic, and lactic acids were also detected. When the temperature was above 255 °C, the formic acid levels decreased, while acetic and lactic acid production increased. The CO_2 formed from the formic acid [17,58]. Moreover, the decarboxylation of amino acids to amines and CO_2 may also be studied as a possible method to produce CO_2 in the HTC of

Table 4
Physicochemical analysis of raw lignocelluloses and sludge and the corresponding hydrochar made from HTC under various hydrothermal parameters.

Feedstock	Proximate analysis			H/C	O/C	Temperature (°C)	Biomass/water (Kg/Kg)	Residence time	Solid yield (wt%)	Proximate analysis			H/C	O/C	References
	FC	VM	Ash							FC	VM	Ash			
Coconut fiber	11.0	80.9	8.1	1.41	0.71	220	10/100	30 min	76.6	24.0	69.8	6.2	1.01	0.37	[134]
						250	10/100	30 min	65.7	27.1	67.9	5.0	0.93	0.30	
						300	10/100	30 min	65.0	42.1	53.6	4.3	0.97	0.21	
						350	10/100	30 min	55.78	38.5	56.6	4.9	0.74	0.21	
Eucalyptus leaves	10.3	79.2	10.5	1.59	0.72	220	10/100	30 min	83.74	20.2	72.5	7.3	1.20	0.38	[134]
						250	10/100	30 min	61.12	23.0	70.1	6.9	1.05	0.37	
						300	10/100	30 min	61.32	31.7	61.2	7.1	1.05	0.25	
						350	10/100	30 min	47.84	33.9	56.2	9.9	1.01	0.22	
Miscanthus	11.7	87.5	0.8	1.54	0.73	190	10/60	5 min	83.5	15.7	83.8	0.5	1.48	0.69	[138]
						225	10/60	5 min	66.9	17.5	81.9	0.7	1.45	0.63	
						250	10/60	5 min	47.8	30.3	68.9	0.8	1.04	0.39	
Empty fruit bunch	15.3	78.7	5.9	1.65	0.82	180	10/10	1 h	–	17.5	78.2	4.3	1.38	0.57	[139]
						200	10/10	1 h	–	24.4	69.7	6.0	1.26	0.49	
						220	10/10	1 h	–	29.5	64.6	6.0	1.20	0.45	
Pine wood meal	12.40	87.31	1.24	1.79	0.77	225	30/90	20 h	–	47.38	51.31	1.31	0.99	0.25	[61]
						245	30/90	20 h	–	49.71	48.89	1.40	0.93	0.24	
						265	30/90	20 h	–	47.15	47.15	1.73	0.90	0.18	
Corncob	17.5.5	81.1 ± 0.5	1.4	1.59	0.67	230	–	6 h	–	31.3 ± 0.3	67.2 ± 0.1	1.5 ± 0.2	1.18	0.41	[140]
cornstalk	–	–	4.64	1.591	0.652	250	10/100	4 h	34.58	54.21	–	4.36	0.935	0.171	[141]
Tamarix ramosissima	–	–	4.36	1.646	0.679	250	10/100	4 h	38.10	58.55	–	0.41	0.896	0.217	
Sugar beet	18.5 ± 0.2	75.4 ± 0.3	6.2 ± 0.2	1.57	0.57	200	20/100	3 h	–	21.2 ± 0.5	66.2 ± 0.4	12.6 ± 0.8	1.05	0.34	[46]
						250	20/100	3 h	–	35.7 ± 1.0	51.8 ± 0.9	12.5 ± 0.2	1.19	0.18	
						250	20/100	20 h	–	38.1 ± 0.2	50.3 ± 0.3	12.0 ± 0.1	1.18	0.18	
Bark	25.5 ± 0.3	66.8 ± 0.4	7.7 ± 0.2	1.26	0.41	200	20/100	3 h	–	35.1 ± 0.3	60.2 ± 1.4	4.7 ± 0.2	1.23	0.32	
						250	20/100	3 h	–	43.2 ± 0.5	50.6 ± 0.3	6.2 ± 0.8	1.03	0.23	
						250	20/100	20 h	–	46.9 ± 0.7	45.2 ± 1.2	7.9 ± 1.9	1.00	0.18	
Corncob residue	17.2	78.6	4.2	1.61	0.78	210	5/50	1 h	–	11.2	83.9	4.8	1.43	0.67	[142]
						210	5/50	2 h	–	23.3	71.4	5.3	1.09	0.50	
						210	5/50	6 h	–	43.5	50.1	6.4	1.00	0.42	
Hyacinth	6.66	52.93	40.41	2.18	0.62	240	6/100	0.5 h	–	–	–	–	1.16	0.45	[62]
						240	6/100	6 h	–	–	–	–	1.11	0.23	
						240	6/100	24 h	–	–	–	–	1.03	0.21	
Wood sawdust	9.5	83.1	7.4	1.67	0.61	200	10/200	30 min	66.8	21.0	72.8	6.2	1.61	0.52	[73]
						250	10/200	30 min	43.8	43.0	49.1	7.9	1.22	0.31	
Bamboo	17.58	80.02	2.40	1.71	0.69	200	10/200	60 min	58.6	20.11	78.09	1.80	1.45	0.57	[143]
						230	10/200	60 min	50.6	28.80	68.90	2.30	1.26	0.43	
						260	10/200	60 min	38.1	44.17	51.73	4.10	0.99	0.25	
Primary sewage sludge	3.90	68.56	27.54	1.89	1.07	140	–	4 h	74.64	1.14	75.97	22.89	1.72	1.07	[125]
						160	–	1 h	81.13	3.30	63.67	33.03	1.83	1.04	
						160	–	2 h	71.08	2.02	66.17	31.81	1.78	1.03	
						160	–	4 h	67.11	1.27	64.33	34.40	1.71	1.04	
						180	–	30 min	70.74	3.53	63.01	33.46	1.74	1.04	
						180	–	1 h	67.18	2.81	63.14	34.05	1.70	1.05	
						180	–	2 h	64.31	1.92	60.44	37.65	1.67	1.06	
						180	–	4 h	61.87	3.46	57.37	39.17	1.63	1.05	
						200	–	15 min	69.32	1.00	63.14	35.87	1.72	1.07	
						200	–	30 min	66.83	1.42	62.30	36.29	1.71	1.06	
						200	–	1 h	64.06	1.18	62.98	35.93	1.65	1.07	
						200	–	2 h	61.26	1.50	60.44	38.07	1.59	1.03	
						200	–	4 h	60.54	5.73	55.33	38.94	1.57	1.01	

(*continued on next page*)

Table 4 (*continued*)

Feedstock	Proximate analysis			H/C	O/C	Temperature (°C)	Biomass/water (Kg/Kg)	Residence time	Solid yield (wt%)	Proximate analysis			H/C	O/C	References
	FC	VM	Ash							FC	VM	Ash			
Sewage sludge	2.66	47.49	49.85	2.02	0.46	180	20/180	30 min	66.18	9.15	22.18	68.47	1.99	0.15	[59]
						220	20/180	30 min	60.58	9.17	18.81	72.02	1.97	0.13	
						260	20/180	30 min	56.23	10.28	27.26	62.46	1.94	0.23	
						300	20/180	30 min	53.00	12.24	16.79	70.97	1.84	0.07	
						260	20/180	60 min	58.51	11.69	23.14	65.17	1.80	0.14	
						260	20/180	90 min	59.37	13.24	24.78	61.98	1.86	0.25	
						260	20/180	6 h	63.32	7.65	22.61	69.74	1.95	0.20	
						260	20/180	8 h	66.19	6.14	34.33	59.53	1.84	0.33	
Anaerobic digestion sludge	7.07	66.87	26.06	1.99	0.90	180	300/300[a]	30 min	93.9	8.37	62.28	29.35	1.77	0.88	[55]
						200	300/300[a]	30 min	92.6	9.30	61.13	29.57	1.72	0.87	
						220	300/300[a]	30 min	88.7	9.50	57.19	33.31	1.56	0.84	
						250	300/300[a]	30 min	80.4	10.70	50.39	38.91	1.23	0.72	
						280	300/300[a]	30 min	80.4	12.70	47.28	40.02	1.01	0.65	
Activated sludge	2.53	76.93	19.31	1.59	0.85	200	30/100	30 min	–	3.54	69.07	26.31	1.17	0.82	[144]
Anaerobic digestion sludge	1.42	69.98	28.60	2.10	0.73	200	–	4 h	53.8	5.47	50.64	43.89	1.60	0.42	[60]
						200	–	6 h	58.2	5.35	50.25	44.39	1.55	0.40	
						200	–	8 h	59.8	6.56	48.76	44.67	1.53	0.41	
						200	–	10 h	60.2	8.00	45.42	46.58	1.53	0.41	
						200	–	12 h	60.4	8.31	45.00	46.69	1.53	0.39	
Paper sludge	3.9	62.1	34.1	1.76	0.67	180	60/60	30 min	–	5.3	62.0	34.3	1.59	0.66	[145]
						200	60/60	30 min	–	5.0	57.8	37.2	1.52	0.64	
						220	60/60	30 min	–	6.5	56.5	37.0	1.44	0.59	
						240	60/60	30 min	–	7.7	56.5	35.8	1.42	0.47	
Paper sludge	10.9	62.1	27.0	1.48	0.64	197	–	30 min	–	10.1	59.4	30.5	1.43	0.58	[145]
Sewage Sludge	4.2	39.3	56.2	2.06	0.50	180	10/100	30 min	77.1	2.8	24.6	72.6	1.98	0.49	[146]
						240	10/100	30 min	70.2	2.2	16.9	81.0	2.23	0.46	
						300	10/100	30 min	66.4	0.8	14.3	84.9	2.18	0.30	
						300	10/100	120 min	65.1	0.1	12.4	87.5	2.24	0.26	

[a] Volume ratio.

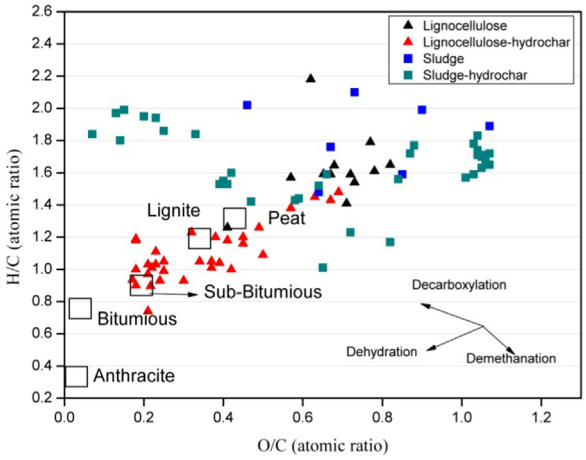

Fig. 12. Van Krevelen diagram for lignocelluloses, sewage sludge and the corresponding hydrochar from different conditions with reference to the data from Table 4. Anthracite, bituminous, sub-bituminous, lignite and peat are shown for comparison.

protein contained in food waste and the protein or amino acids in SS. Other possible methods of CO_2 formation may result from condensation reactions as well as the cleavage of molecular bonds in the degradation of biomacromolecules.

4.2. Surface functionality characterization

The structural characteristics of hydrochar derived from different feedstock types and process conditions are extremely different. Due to the complex composition of the hydrochar, coupled with the very complicated variations of hydrothermal parameters and feedstock used in HTC, FTIR techniques are employed in most studies to analyze the surface functional groups of raw biomass and hydrochar. The FTIR spectra can provide a mechanistic investigation of the evolution of hydrochar, and many studies have used this technique to analyze the structural transformation in the different HTC conditions of various biomass sources, including coconut fiber and dead eucalyptus leaves [134], miscanthus [147], barley straw [148], pinewood [149], switchgrass [150], and SS [151]. The typical FTIR spectrum response to the raw biomass and hydrochar from lignocellulose biomass and SS are shown in Fig. 13.

Compared to the feedstock, the O-H stretching vibrations in the hydroxyl or carboxyl groups presented in hydrochar showed obvious weakening, and this diminishment is generally attributed to the dehydration that occurred during HTC [55,140,144,152–154], which was consistent with the reduction in the H/C and O/C ratios observed in the Van Krevelen diagram. However, unlike the paper sludge, the hydroxyl functional group in the paper sludge showed no significant change during the HTC process due to thermo-mechanical or thermo-chemical pretreatment in the pulping process [155]. Furthermore, the decrease of the hydroxyl content in hydrochar would lead to an increase in hydrophobicity, which is critical to fuel storage, handling, and resistance to humidity when used for solid fuel applications [134]. Peaks that correspond to stretching vibrations of aliphatic CH_x are stronger in the hydrochar as compared to raw biomass; for example, coconut fiber and dead eucalyptus [134], eucalyptus sawdust and barley straw [153], husks of nuts of Carya cathayensis Sarg [76], palm shell [152], corn stalks [156], SS [60], and anaerobically digested sludge [55]. This suggests that the breakup of polymeric substances in the HTC process would result in the appearance of aliphatic structures in hydrochar, while the appearance of aromatic C-H out of plane bending vibrations suggested that hydroaromatic structures emerge after HTC. The C=C stretching in the lignocellulose suggests that aromatic groups in lignin become weaker, due to the incomplete decomposition associated with $-OCH_3$ groups decomposed by deoxygenation reactions, intermediate aromatic structures formed from keto-enol tauomerism of dehydrated species, or from intramolecular dehydration of the oligosaccgaides or monosaccharides [53,134]. Cellulose is often compared with lignocellulose in the HTC process because of their similar FTIR spectrum to explain the chemical structure changes of hydrochars. For example, in Liu et al. [53], a new band corresponding to the C=C vibrations in the aromatic skeleton was observed, which revealed that the aromatization of hydrochars derived from poplar tree wood occurred during the hydrothermal reaction similar to cellulose. Their finding was also consistent with Sevilla's [157] study. Yu et al. [158] studied the HTC materials obtained using four different precursors, namely xylose, glucose, sucrose, and starch; their results supported the concept of an aromatization skeleton for biomass during hydrothermal treatment. Different to lignocellulose, the C=C stretching in hydrochars produced from SS provides significant evidence for the increased presence of aromatic ring carbons resulting from aldol condensation and aromatization reactions [43,60]. However, this is contrary to the findings of Kim et al. [55], who found that the intensity of the peaks of C=C bonds for the hydrochars decreased as temperature increased, which could be attributed to the fact that the SS analyzed had been digested.

However, the oxygenated functional groups contained in hydrochars are an important characteristic for the ease and ability to produce hydrochar during HTC. Gao et al. used waste eucalyptus bark in the HTC, and showed that the stretching of C=O in ketone, amide, and carboxylic groups generally decreased in the hydrochar because the occurrence of decarboxylation increased with the residence time. The same result was found during the HTC of barley straw; C=O stretching

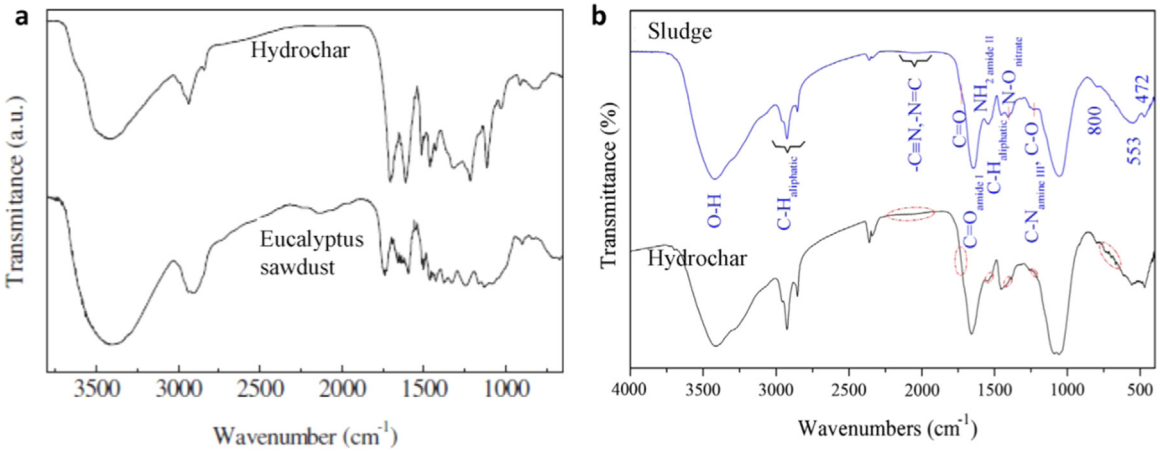

Fig. 13. Typical FTIR spectrum of the lignocellulose, SS and corresponding hydrochar [144,148].

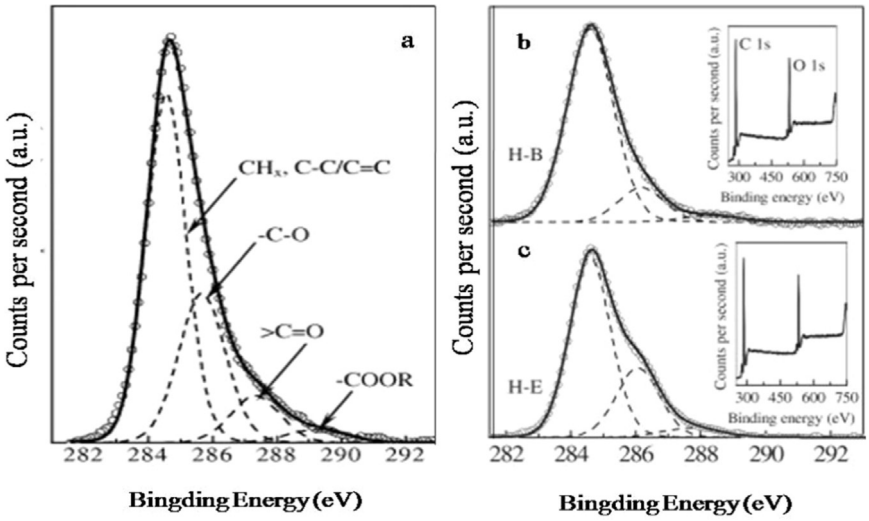

Fig. 14. C1s core level spectrum of hydrochar derived from (a) pure cellulose at 250 °C, (b) barley straw, and (C) eucalyptus sawdust at 250 °C [148].

vibrations were attributed to non-conjugated keto-carbonyl groups which nearly disappeared [153]. In another paper, the C=O stretching vibrations were not present after HTC due to the degradation of carboxyl and acetyl groups in hemicellulose of both corn cob and miscanthus; however, an intense peak at another wavenumber ascribable to C=O vibrations of carbonyl, quinone, ester, or carboxyl groups was observed in the hydrochar spectra [140]. This may be attributed to the dehydration of water from the equatorial hydroxyl groups in the monomers derived from cellulose [53]. Regardless of whether SS was digested, the stretching vibration of C=O as ketone and amide groups or asymmetric stretching in carboxylic groups also decreased due to decarboxylation reactions occurring, which resulted in the conversion of the carbon compounds into CO_2 [55,60,145]. However, Zhao et al. [144] found that the C=O stretching of ester carbonyl groups disappeared in the hydrochar spectra caused by the derosination reaction. This difference between lignocellulosic materials and SS indicates that the occurrence and the reaction severity of decarboxylation, unlike dehydration, are heavily dependent on the natural materials in the HTC. The C-O-C vibration in the lignocellulose generally exhibits noteworthy weakening due to the degradation of cellulose or lignin where the characteristic aromatic structure is generally preserved in the HTC process. In the HTC of SS, the C-O-C stretch may also be considered as asymmetric stretching in aliphatic ether, or the characteristic peak of the derivatives of polysaccharides which decompose into short-chain derivatives of saccharides that reduce due to the cleavage of C-O-C at higher temperatures. The hydrochar also retains a higher amount of oxygen functional groups contained in the C-O stretching vibrations in hydroxyl, ester, or ether, coupled with the O-H bending vibrations and C=O mentioned above. For the incomplete decomposition of lignin, the aromatic C-O stretching bands stretching in -OCH_3 groups in the hydrochar can observed in many studies [154,159,160]. In a study of the HTC process of SS, He et al. observed that a drastic increase of relative intensity was due to -C-O-R in aliphatic ethers and alcohol -C-O stretching [60,161]. This result is in contrast to the anaerobically digested SS used in the HTC which showed that the decarboxylation reaction caused the decrease of C-O [55].

Differing from lignocellulose, the surface functional characterization of SS derived hydrochar is generally similar; the existence of N-rich functionality is due to natural properties and higher protein content. FTIR was also performed to study the N functional group contained in the sludge and the corresponding hydrochar by Zhao et al. [144]. As shown in Fig. 13, the FTIR spectrum of the SS and the derived hydrochar were adopted to illuminate the change in N. The N functional group in the spectrum showed amide groups at 3420 cm^{-1} (N-H stretching); 1656 cm^{-1} (amide I band), and 1540 cm^{-1} (amide II band), which indicates a significant protein content in the SS. The amide II band shifted and became weak during degradation and protonation, 1228 cm^{-1} attributed to the C-N stretch vibrations by amide III (tertiary amine), while similar performance was observed at the broad band around 2090 cm^{-1} assigned to nitrile (-C≡N) and isonitrile (-N = C) stretching; however, the amide I and amide III bands were overlapped by the C=O vibration of carboxylates and C-O vibration of carboxylic acids, respectively [144]. Furthermore, the band at 1404 cm^{-1} attributed to the N-O binding in nitrite observed in the SS vanished in the spectra for the dissolution of nitrite, and a similar peak corresponding to the N-O group was observed in raw sludge, but decreased in the spectra of the HTC of digested SS in the study by Kim et al. [55].

The surface functionality presenting on the outer surface of hydrochar can also be analyzed by employing XPS. For hydrochars derived from lignocellulose, two main peaks in C (C1s) at around 285 eV and O (O1s) at around 530 eV are usually observed in the XPS wide-scan spectrum [162]. For the C1s envelope, different binding energies were attributed to C−C, C=C, C−HX, C−O, C=O, and COO stretches; however, the O1s envelope peaks at different binding energies can be ascribed to O=C and O−C stretches. Additionally, the spectra of high resolution XPS of C1s and O1s are used to quantify the carbon and oxygen forms on the hydrochar surface [162]. Research by Sevilla et al. [148] obtained hydrochar from the HTC of eucalyptus sawdust and barley straw under 250 °C. Their XPS results showed that hydrochar products had rich oxygenated groups on the surface, although the proportion of some oxygenated groups including hydroxyl groups, carbonyl groups, and esters differed based on the nature of the biomass. Representative C1s core level spectrum of hydrochar derived from eucalyptus sawdust, barley straw, and pure cellulose are shown in Fig. 14. The atomic ratios (O/C) analyzed by elemental analysis (0.269 and 0.200 for eucalyptus sawdust and barley straw, respectively) were compared with the result from XPS (0.318 and 0.298 for eucalyptus sawdust and barley straw, respectively) and results indicated that oxygen had accumulated at the periphery of the hydrochar particles which lead to a higher oxygen content as compared to the inner section. This was attributed to the cellulose being extracted from the lignocellulosic body and subsequently deposited on the outer surface which contained products of the incomplete degradation of lignin [148]. This result was supported by another study which determined that the XPS spectra of hydrochar microspheres derived from pure cellulose possess higher concentrations of oxygen in the outer layer as compared to the core of the particles. This is also indicated by the

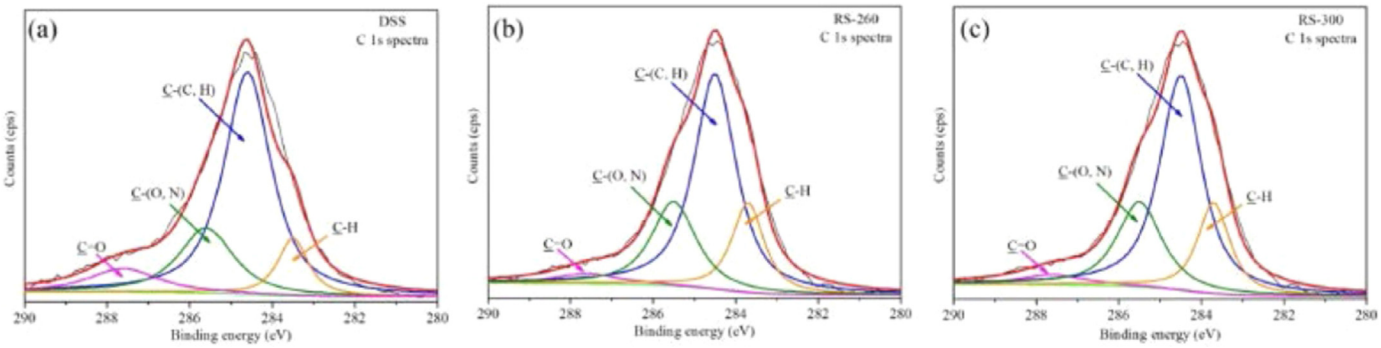

Fig. 15. C1s core level spectrum of hydrochar derived from (a) SS and hydrochar from (b) 260 °C and (c) 300 °C respectively [163].

comparison of the (O/C) atomic ratios determined by elemental analysis (0.239 and 0.254 for the samples produced at 250 °C for 4 and 2 h, respectively) with those calculated by XPS (0.282 and 0.275, respectively) [53]. The analysis also showed that the oxygen groups present in the core of the particles formed with stable groups (i.e. ether, quinone, pyrone, etc.), differing from those in the outer layer which consist of more hydrophilic groups (i.e. hydroxyl, carbonyl, carboxylic, ester, etc.) [53]. A similar result was also found by Xiao et al. [141], who investigated the XPS spectra of hydrochar derived from two lignocellulosic biomass sources; corn stalk and Tamarix ramosissima [141].

The SS derived hydrochar also demonstrated higher (O/C) atomic ratios in the outer layer as compared to the inner core. For example, in a study by He et al. [163], hydrochar prepared at 260 °C and analyzed by XPS (Fig. 15) showed 0.28% of O/C, higher than the ultimate analysis result of 0.547. Meanwhile, as shown in Fig. 15, the C1s around 285.6 ev corresponding to C-(O, N) showed slight increases from 20.32% to 22.81% and 23.10% for 260 °C and 300 °C derived hydrochar, confirming the high concentration of oxygenated groups on the surface of the hydrochar particle. However the C=O at approximately 287.6 ev showed a large decrease due to decarboxylation [163].

In summary, these results are consistent with the FTIR spectrum which indicates the presence of both aromatic and aliphatic carbon with more oxygen-rich functional groups on the surface of hydrochar reflected by XPS. The hydrochar exhibits high stability aromatic structures as a basic building block mixed with aliphatic carbons and retains a certain amount of oxygen functional groups.

4.3. Aromatic structure characteristics

Solid state ^{13}C magic angle spinning NMR has been employed as a valuable characterization technique for comparisons without the need for peak ratios, identifying the amorphous material that provides valuable complementary data to the surface functionality analysis. Each resonance peak quantified in relation to the total resonance intensity can provide the relative abundance of individual molecular groups [162,164]. Liu et al. [134] conducted the ^{13}C NMR spectra of hydrochar obtained from coconut fiber at temperatures from 220° to 375°C (Fig. 16**)**. The hydrochars obtained at low temperatures (220–250 °C) showed a marked decrease at 73 ppm (the C2, C3, and C5 of carbohydrate) as a representative of both cellulose and hemicellulose. A similar tendency was also observed at the peak of 105 ppm, accounting for cellulose C-1, and the peak around 102 ppm, ascribed to hemicellulose. The peak ascribed to lignin in the range of 116–154 ppm and 55 ppm (methoxyl group) remained invariable until 300 °C and the aromaticity of hydrochars increased above 300 °C [134]. These results indicate that the HTC had decreasing aliphaticy, which virtually disappeared above the critical point, and the increasing aromaticity of hydrochars with hydrothermal temperature increases [134]. Cao et al. [46] investigated bark hydrochars at 200–250 °C for 3 and 20 h, respectively. Quantitative chemical compositions of feedstock and hydrochar obtained from ^{13}C DP/MAS NMR spectra showed the hydrochar was enriched with 27% aromatic C compared to the 9% in the feedstock at the spectral range of 112–140 ppm, and an increase in alkyl and carbonyl C. Their findings indicated that HTC resulted in almost total reduction of carbohydrate and formation of aromatic structures, whilst the lignin structures were altered slightly in the bark hydrochar at 250 °C [46]. Fuertes et al. [165] investigated both cross polarization (CP) and direct polarization spectra of corn stover derived hydrochar at 250 °C for 4 h. A strong peak in the aromatic region at approximately 129 ppm along with a sharp peak at 147 ppm were ascribed to the aromatic C in lignin and two dominant peaks were observed in the alkyl region at 56 and 35 ppm due to the methoxyl C associated with lignin structures and C- and H-substituted alkyl C, respectively [165]. Furthermore, the potential signal of aromatic C detected in both techniques for hydrochars were approximately equal. Zhang et al. [151] analyzed the CPMAS^{13}C NMR of hydrochar derived from municipal SS at 190–260 °C with a residence time from 1 to 24 h. Their analyses also indicated that aromaticity was markedly enhanced with an increase of 41%. Conversely, there was a decrease in aliphaticity of at least 45% and 31% for Oalkyl C and carboxyl C, respectively, observed when the reaction severity increased [151]. He et al. [163] (Fig. 16) showed that an increase in hydrothermal temperature resulted in an increase of the aromatic C-C (110–160 ppm). Temperatures from 200° to 340°C resulted in relative intensities from 16.15% to 32.11%, which were all higher than the raw sludge. The aromatic C-O (145–160 ppm) showed an increased tendency, which was in accord with the XPS confirming that oxygen-rich functional groups may connect with the aromatic structure on the outer layer [163]. In summary, the NMR spectra can be divided in to aliphatic and aromatic regions by the degree of carbon saturation. Thus, weakness in the aliphatic region and formation or enhancement in the aromatic region may provide evidence of the apparent coalification of HTC [134,166].

In conclusion, all the structures suggest the existence of aromatic characteristics in hydrochar, even when the skeleton is constructed with benzene rings. Furthermore, the difference in the structural characteristics of the hydrochar heavily depend on the hydrothermal conditions employed in the HTC, especially temperature. Hence, the basic aromatic motif is generally accepted for the hydrochar skeleton.

4.4. Morphological and textural character

The morphology of hydrochars under different HTC conditions are generally studied by SEM which provides micrographs showing the physical properties and surface morphology. In the first chapter, we discussed the microsphere characteristics of model chemicals under different hydrothermal conditions; however, the hydrochar of raw biomass must exhibit a more complex morphological characterization. Generally, hydrochar shows a coarser surface as compared to the smooth character of raw biomass. As mentioned previously, more easily

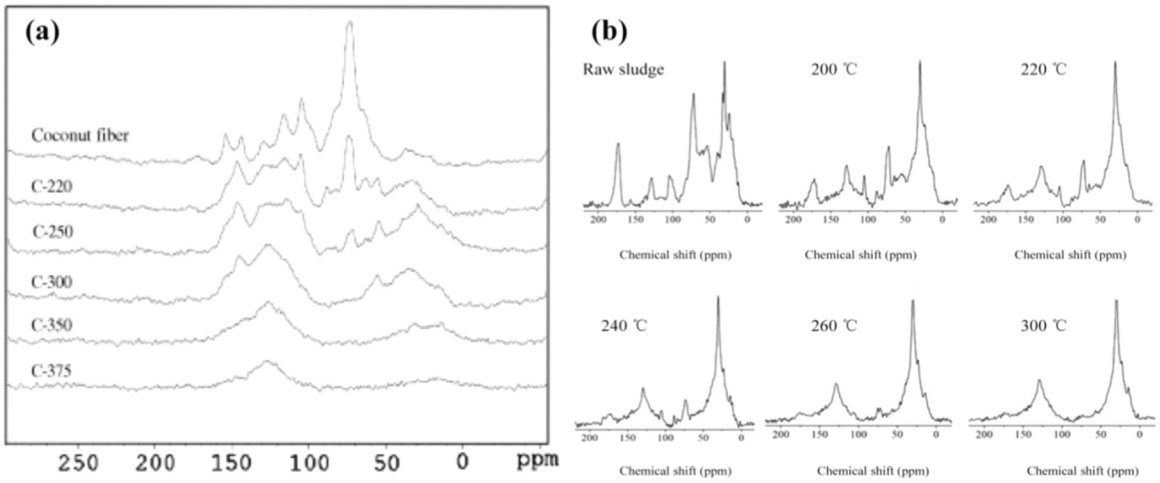

Fig. 16. ^{13}C NMR spectra of (a) coconut fiber and coconut fiber derived-hydrochar obtained from different hydrothermal temperatures [134]; (b) raw sludge and corresponding hydrochar obtained from different hydrothermal temperatures [163].

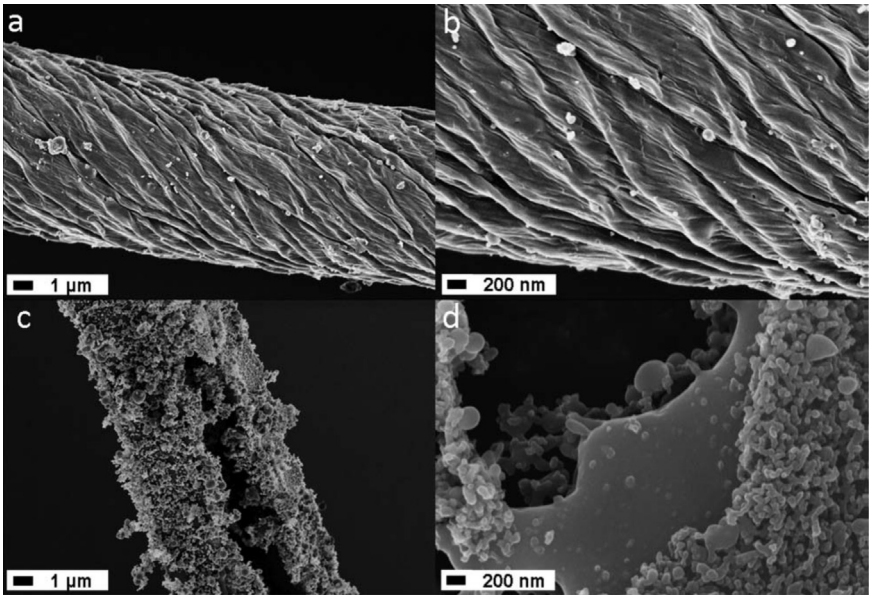

Fig. 17. SEM images hydrochar from rye straw under 160 °C (a, b) and 240 °C (c, d) [64].

collapsible polymers, such as hemicellulose, can more easily decompose into fragments that lead to a rugged and even porous surface on the solid residue. These small fragments would then further melt or form carbonaceous spheres on the surface. Xiao et al. [141] compared SEM images of the feedstock of corn stalk and Tamarix ramosissima and their derived hydrochars, and results showed that the raw materials possessed a relatively continuous and flat smooth surface; however, irregular and rougher surfaces were observed, and new microsphere structures formed with different shapes and sizes on the hydrochar surface. The formation of agglomerated particles showed that degradation of cellulose contained in the plant wall took place. Nevertheless, the main structure remained for HTC performed at relatively low temperatures; thus, the decomposition of lignin requires higher carbonization temperatures during the HTC process. Falco et al. [64] investigated the SEM of hydrochars from rye straw under temperatures from 160° to 240°C. Their results (Fig. 17) showed that particle formation took place on the surface of the raw straw fibers which is similar to cellulose, but contrasts with the generally homogeneous distribution of hydrochars derived from glucose. The body of raw straw maintained its original structural scaffold due to the presence of higher temperature resistant lignin, and the cellulose may also undergo reactions having the characteristics of a pyrolysis-like process [64].

The same characteristics also can be observed in the SEM images (Fig. 18) of SS and its corresponding hydrochar. Untreated SS presents a relatively smooth surface with limited porosity. Gai et al. [167], found that a significant amount of porous structure appeared on hydrochar surface, and the microstructure of the hydrochar markedly differed from the SS. This indicates that the decomposition of organic components occurred during the HTC. Simultaneously, micrometer sized particle dispersions with various forms such as honeycombs, fluffy sponges, or spherically shaped particles were observed on the surface by the SEM, and their formation was mainly attributed to the carbohydrates [167].

Regarding textural characterization, pore size distribution and specific surface area are generally used to analyze the textural changes of hydrochar. These physical properties are critical to the soil aeration of beneficial solid organisms when hydrochar is applied to soil [27]. To investigate these properties, N_2 adsorption at 77 K and CO_2 adsorption at 273 K are frequently used [162,168]. Based on the N_2 adsorption isotherms, the S_{BET} equation can deduce the specific surface area, and micropore volume can be estimated using the Dubinin – Radushkevich method. Furthermore, by analyzing differences between the adsorption

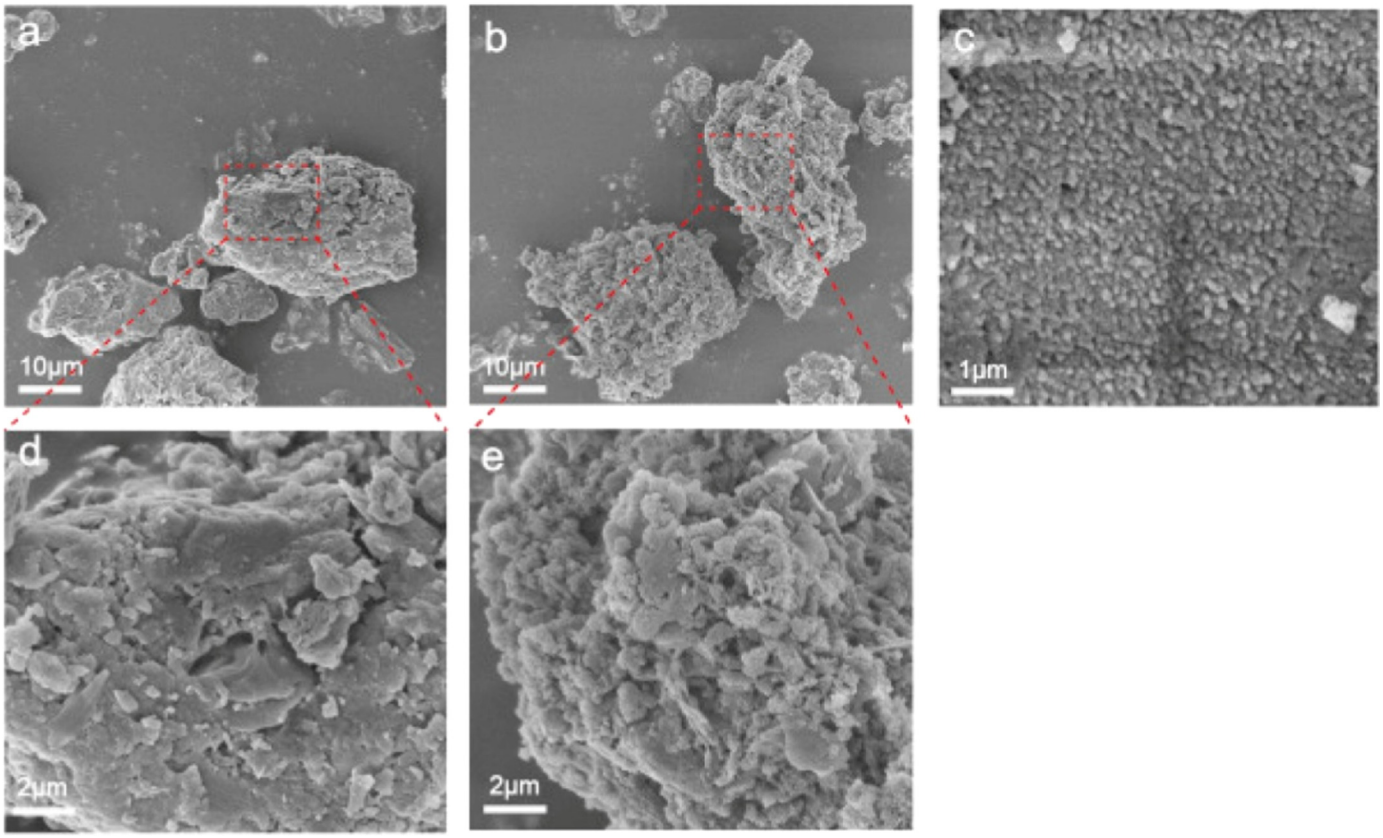

Fig. 18. SEM image of sewage sludge (a) 10 μm and (d) 2 μm, hydrochar (b) 10 μm, (c) 1 μm and (e) 2 μm of sewage sludge [167].

Table 5
General determination methods for structural compounds of hydrochar.

Items	Hydrochar characterization	Chracterization methods
Elemental composition	Ratio of C, H,O, N, S etc.	Elemental analyzer, XPS, EDS
Physical structure	Morphology features	SEM,TEM
	Porous performance	N_2 ads.-des,
Chemical state	Surface functionality	XPS, FT-IR
	Aromatic structure	Solid ^{13}C NMR,
	Metallic contents	XRD
	Degree of carbonaceous ordering and crystallinity	Raman

volume of N_2 at a relative pressure of 0.95 and micropore volume, the volume of mesopores can be determined [169]. The Dubinin−Radushkevich method is also used to estimate narrow micropore volume according to the CO_2 adsorption isotherms [162]. However, it is generally accepted that hydrochars have poor micro-porosity and low surface area, and their textural characteristics and stability depend on the feedstock and conditions used in HTC [27]. Here, we do not show the information on the pore size distribution and specific surface area because many reviews provide this information. Readers can refer to some excellent specific review articles or book chapters, including [27,29]. However, there are limited studies regarding the application of hydrochar as soil an additive. Although the soil ecology and inhabiting microorganisms can be altered by hydrochar addition, hydrochar can have uncertain effects on plant biomass [170]. Adverse effects on germination and growth were attributed to the phytotoxic volatile components contained in hydrochar [171,172]. Bargmann et al. [172] found that compounds including guaiacol, levulinic acid, glycolic acid, acetic acid, glycolaldehyde dimer, and catechol had a negative impact on cress seed growth. Fang et al. [173] found that the washed hydrochars made from plant biomass showed no significant influence on the seed germination rate of brown top millet; however, hydrochar from low temperatures (200 °C) have some effect on the root development of seedlings not seen in hydrochar from higher temperatures (250 and 300 °C). The phenomenon were attributed to unknown factors, such as the reduction of volatile matter and water insoluble-compounds at high temperatures. Additionally, a decrease in plant available N caused by nitrogen immobilization was also suggested as a possible cause [174]. Similarly, Bargmann et al. [175] showed that hydrochar reduced the mineral N in soil; however, the hydrochar aging process was beneficial to reduce the negative effects and nitrogen immobilization. Hence, it can be concluded that appropriate pre-treatments such as washing or storage to remove the phytotoxic volatile components are also necessary. However, to date, a systematic study on the textural characteristics and the application of hydrochar to soil are not fully understood; extensive work needs to be done in this field. Based on previous studies and reviews, the general determination methods of the structural compounds of hydrochar are summarized in Table 5.

5. Energy balance

The HTC process has the capability to convert biomass waste into lignite-like solid fuel; hence, it is necessary to provide an assessment of the energy balances of the HTC process. Many studies have reported that HTC is an exothermic process [17,176]. To maximize the energy yield, it is necessary to recover the released energy and hydrochar can usually be consumed directly as a solid fuel or through blend-combustion with coal [177]. Danso-Boateng et al. [176] studied the HTC process energetics using human fecal waste and stated that the efficiency of recycled energy could be affected by changing the feedstock containing solids 15–25%. Furthermore, energy recovered from flashing off steam and hydrochar combustion were sufficient for the entire HTC process, including drying off the moisture within hydrochar without using external energy. Thus, biomass with a high moisture

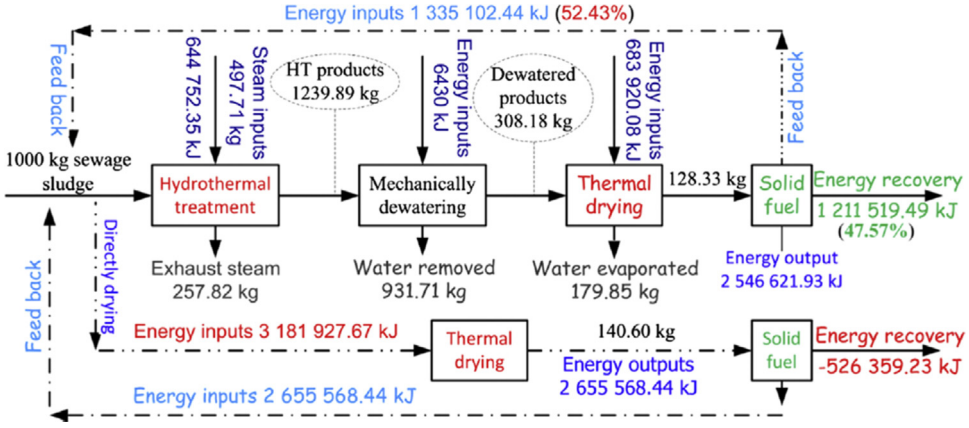

Fig. 19. Typical energy balance of HTC of SS producing hydrochar as solid fuel [12].

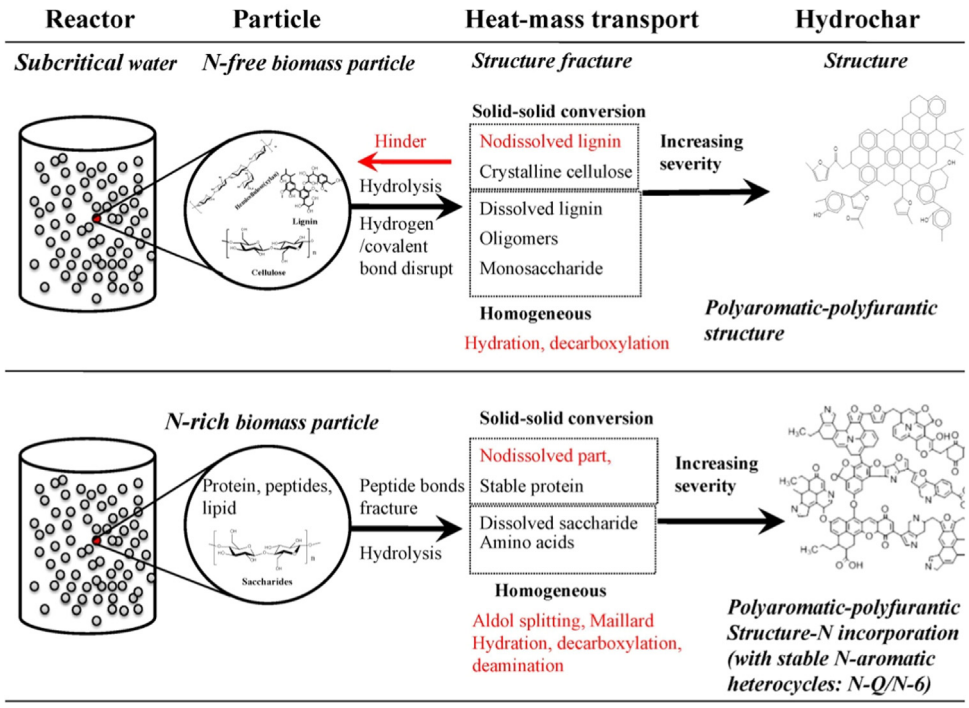

Fig. 20. A concise summary of hydrochar formation ways from N-rich or N-free content biomass.

content may be not sustained by the energy recovery from the HTC process. Zhai et al. [178] estimated the energy balance during HTC of lignocellulosic biomass and SS blends, and indicated that the energy recovery rate followed the species of lignocellulosic biomass in the order corncob > cornstalk > sawdust > rape straw, and an SS/corncob blend at 300 °C with a 60 min residence time was suggested as the best condition to produce hydrochar with an energy recovery rate of approximately 71.60%. Zhao et al. [12] evaluated the energy balance of HTC of SS at 200 °C with a 30 min residence time and found that approximately 47.6% of the energy derived from hydrochar combustion could be recovered as heat or power, while the remaining 52.4% was sufficient for running the HTC, mechanical dewatering, and the drying process. A typical energy balance for HTC producing hydrochar as solid fuel is illustrated in Fig. 19 [12]. The energy efficiency of HTC was also compared with the conventional thermal drying process, which requires additional fuel at the rate of 5.3 MJ for 1 t of sludge (85.94% water content). Thus, it can be concluded that the energy recovery and balance during HTC depends on the feedstock and hydrothermal conditions, such as initial moisture and operating processes. Understanding the energy balance of HTC also provides a reference for economic investments and commercial applications. Wirth et al. [179] estimated the influence of plant capacity, feedstock choice, and supply logistics on production, and suggested that biomass supply is the dominant cost as opposed to transformation cost. Furthermore, Reza et al. [26] indicated that the total capital investment during HTC depended mainly on the plant capacity and feedstock, while waste biomass like SS and municipal organic waste were attractive because additional revenues could generated if facilities were paid to take the resource [26]. Recently, a commercial demonstration of HTC using non-segregated MSW for solid fuel production was established in Indonesia [180]. Researchers estimated the energy balances and suggested that hydrochar prepared at 220 °C with a residence time of 30 min producing 15% hydrochar, were sufficient to supply energy requirements, while the running costs of HTC were low [180]. In spite of these findings, the industrialization and large-scale application of HTC still faces challenges, and further research and evaluation are vital to establish HTC as an environmentally sustainable utilization of waste biomass.

6. Conclusions

In this review, the hydrothermal variables that play a critical role in hydrochar formation were investigated, and details of the physicochemical analysis including proximate analysis or ultimate analysis, surface functional groups, aromatic structure and morphological characteristics were also reviewed. The formation mechanism of hydrochar during the HTC process of two representative biomass sources, lignocellulose and sludge (N-free and N-rich biomass sources, respectively) was investigated for single composition conversion and real biomass, as shown in Fig. 20.

The literature reviewed in this study indicates the significant differences in the characteristics of hydrochar under various parameters. Hydrochar products differ based on the origin biomass and hydrothermal variables. An increase in hydrothermal severity (temperature and/or residence time) leads to the generation of hydrochar with higher condensed carbon through the removal of H and O in a coalification-like process. The components of raw biomass go through various degradation processes during HTC; however, intermediate chemicals derived from biomass in subcritical water, and a combination of solid–solid conversion are regarded as the major hydrochar formation mechanisms. The major components of waste biomass were highlighted for a better understanding of the underlying reactions, and the interactions of the components in real biomass conversion during the degradation process. The N- rich biomass (containing protein) introduced N into the hydrochar, which evolved into a more stable form and was incorporated into the hydrochar structure in a nitrogen-containing aromatic network (pyridinic-N and quaternary-N) as the hydrothermal severity increased. The surface chemistry of the hydrochar exhibited increasingly stable aromatic structures containing a mixture of aliphatic carbons with oxygen functional groups. The basic hydrochar structure is generally accepted to be comprised of an aromatic network combined with furanoic compounds connected via aliphatic bridges. However, the formation of the structure is dependent on both the hydrothermal conditions, which determine whether the pyrolysis-like process or intermediate polycondensation reaction pathway dominates, and the raw feedstock (N-rich or N-free). Based on our discussion on hydrochar production, formation mechanisms, and structural or morphological explorations, the crucial properties of hydrochar can be better understood.

7. Future perspectives

According to the literature summarized in this review, progress has already been made towards understanding hydrothermal conversion, hydrochar formation mechanisms, and hydrochar characteristics. In all cases, hydrochar was a sustainable alternative for the utilization of high moisture waste biomass. However, scientific and technological challenges remain before the chemical mechanisms behind the hydrothermal conversion of biomass and hydrochar structure can be fully understood. This data is vital to facilitate more extensive production and applications of hydrochar. Several research gaps are detailed as follows:

(1) A larger range of organic substances contained in waste biomass, including carbohydrates, proteins, lipids, and polyphenols require investigation to determine their conversion mechanisms during HTC. Research efforts need to address the heterogeneity of raw biomass to determine the multiple influences caused by such a great diversity of components. On the other hand, further studies are needed to analyze the effect of large variations in raw biomass; both on hydrochar production and degradation behaviors.
(2) Temperature was identified as a critical parameter governing the characteristics of hydrochar. In addition to the hydrothermal conditions reviewed in this paper, more variables require consideration; for example, the heating rate, particle size, concentration of substrate, packing ratio, catalysis addition, and liquid quality. Detailed parameters should be developed for the specific characteristics of hydrochar based on these variables. These data would aid in improving conversion efficiency and provide reference data for industrial scale design and production, particularly because industrial scale production faces challenges with respect to high pressures, solid–liquid separation heat transfer and recovery, and water recirculation. It is necessary to develop reaction models to analyze these process parameters to evaluate their influence in both lab-scale and industrial-scale experiments.
(3) While the HTC of biomass can be successfully utilized for the conversion of biomass to hydrochar, literature on the detailed formation mechanisms of hydrochar remain unclear and are confined to the degradation of pure chemicals. Hence, further research is needed to elucidate the mechanisms of hydrochar formation from complex biomass In particular, the conversion mechanisms of N-rich biomass are not yet fully understood. Furthermore, the presence of inorganic species in biomass, including K, Ca, Na, Mg, and heavy metals can also alter the formation behavior of hydrochar. The elucidation of these mechanisms will help to control the production, composition, and characteristics of hydrochar.
(4) In spite of a large number of studies on the hydrochar these years, the liquid and gas product receive limited concern and these by-products containing intermediate products need more detail analysis for better understanding the hydrothermal conversion process in relation to the hydrochar formation and this shows equal importance for the theoretical basis. In addition, post-treatment process is essential to HTC process water and hydrochar for the recovery of nutrient substance such as N, P. Qualitatively and quantificationally work need to be promoted for the distribution, transformation mechanism and recovery, and future efforts should take relevant analysis and treatment into more account.

Acknowledgements

This research was financially supported by the project of National Natural Science Foundation of China (Nos. 51679083), the Interdisciplinary Research Funds for Hunan University (2015JCA03). The authors state that the permission for any copyrighted figures is attained.

References

[1] Chew JJ, Doshi V. Recent advances in biomass pretreatment – Torrefaction fundamentals and technology. Renew Sustain Energy Rev 2011;15:4212–22.
[2] Hastings A, Clifton-Brown J, Wattenbach M, Mitchell CP, Stampfl P, Smith P. Future energy potential of Miscanthusin Europe. GCB Bioenergy 2009;1:180–96.
[3] Hillier J, Whittaker C, Dailey G, Aylott M, Casella E, Richter GM, et al. Greenhouse gas emissions from four bioenergy crops in England and Wales: integrating spatial estimates of yield and soil carbon balance in life cycle analyses. GCB Bioenergy 2009;1:267–81.
[4] Akhtar J, Amin NAS. A review on process conditions for optimum bio-oil yield in hydrothermal liquefaction of biomass. Renew Sustain Energy Rev 2011;15:1615–24.
[5] Menon V, Rao M. Trends in bioconversion of lignocellulose: biofuels, platform chemicals & biorefinery concept. Prog Energy Combust Sci 2012;38:522–50.
[6] Appels L, Baeyens J, Degrève J, Dewil R. Principles and potential of the anaerobic digestion of waste-activated sludge. Prog. Energy Combust Sci 2008;34:755–81.
[7] Zhou Y, Zhang Z, Zhang Y, Wang Y, Yu Y, Ji F, et al. A comprehensive review on densified solid biofuel industry in China. Renew Sustain Energy Rev 2016;54:1412–28.
[8] Wang T, Zhai Y, Zhu Y, Peng C, Xu B, Wang T, et al. Influence of temperature on nitrogen fate during hydrothermal carbonization of food waste. Bioresour Technol 2018;247:182–9.
[9] Zhao P, Shen Y, Ge S, Chen Z, Yoshikawa K. Clean solid biofuel production from high moisture content waste biomass employing hydrothermal treatment. Appl Energy 2014;131:345–67.
[10] Chandra R, Takeuchi H, Hasegawa T. Methane production from lignocellulosic agricultural crop wastes: a review in context to second generation of biofuel production. Renew Sustain Energy Rev 2012;16:1462–76.
[11] Moreno AD, Ibarra D, Alvira P, Tomás-Pejó E, Ballesteros M. A review of biological delignification and detoxification methods for lignocellulosic bioethanol

production. Crit Rev Biotechnol 2014;35:342–54.
[12] Zhao P, Shen Y, Ge S, Yoshikawa K. Energy recycling from sewage sludge by producing solid biofuel with hydrothermal carbonization. Energy Convers Manag 2014;78:815–21.
[13] Die FB. Knapp W, editor. Anwendung hoher Drücke bei chemischen Vorgängen und eine Nachbildung des Entstehungsprozesses der Steinkohle. Halle a. d.Saale: Wilhelm Knapp; 1913. p. 18.
[14] Karayıldırım T, Sınağ A, Kruse A. Char and coke formation as unwanted side reaction of the hydrothermal biomass gasification. Chem Eng Technol 2008;31:1561–8.
[15] D.W vK. Graphical-statistical method for the study of structure and reaction processes of coal. Fuel 1950;29:25.
[16] Knez Ž, Markočič E, Hrnčič MK, Ravber M, Škerget M. High pressure water reforming of biomass for energy and chemicals: a short review. J Supercrit Fluids 2015;96:46–52.
[17] Funke A, Ziegler F. Hydrothermal carbonization of biomass: a summary and discussion of chemical mechanisms for process engineering. Biofuels Bioprod Bioref 2010;4:160–77.
[18] Wiedner K, Naisse C, Rumpel C, Pozzi A, Wieczorek P, Glaser B. Chemical modification of biomass residues during hydrothermal carbonization – What makes the difference, temperature or feedstock? Org Geochem 2013;54:91–100.
[19] Xu Q, Qian Q, Quek A, Ai N, Zeng G, Wang J. Hydrothermal carbonization of macroalgae and the effects of experimental parameters on the properties of hydrochars. ACS Sustain Chem Eng 2013;1:1092–101.
[20] Saidur R, Abdelaziz EA, Demirbas A, Hossain MS, Mekhilef S. A review on biomass as a fuel for boilers. Renew Sustain Energy Rev 2011;15:2262–89.
[21] Chandra R, Takeuchi H, Hasegawa T, Kumar R. Improving biodegradability and biogas production of wheat straw substrates using sodium hydroxide and hydrothermal pretreatments. Energy 2012;43:273–82.
[22] Tommaso G, Chen W-T, Li P, Schideman L, Zhang Y. Chemical characterization and anaerobic biodegradability of hydrothermal liquefaction aqueous products from mixed-culture wastewater algae. Bioresour Technol 2015;178:139–46.
[23] Passos F, Ferrer I. Influence of hydrothermal pretreatment on microalgal biomass anaerobic digestion and bioenergy production. Water Res 2015;68:364–73.
[24] Titirici M-M, White RJ, Falco C, Sevilla M. Black perspectives for a green future: hydrothermal carbons for environment protection and energy storage. Energy Environ Sci 2012;5:6796.
[25] Judy A, Libra KSR, Claudia Kammann, Axel Funke, Berge Nicole D, Neubauer York, Maria-Magdalena Titirici CF, Bens Oliver, Kern Jürgen, Emmerich Karl-Heinz. Hydrothermal carbonization of biomass residuals: a comparative review of the chemistry, processes and applications of wet and dry pyrolysis. Biofuels 2011;2(1):89–124.
[26] Reza MT, Andert J, Wirth B, Busch D, Pielert J, Lynam JG, et al. Hydrothermal carbonization of biomass for energy and crop production. Appl Bioenergy 2014;1.
[27] Kambo HS, Dutta A. A comparative review of biochar and hydrochar in terms of production, physico-chemical properties and applications. Renew Sustain Energy Rev 2015;45:359–78.
[28] Okajima I, Sako T. Energy conversion of biomass with supercritical and subcritical water using large-scale plants. J Biosci Bioeng 2014;117:1–9.
[29] Jain A, Balasubramanian R, Srinivasan MP. Hydrothermal conversion of biomass waste to activated carbon with high porosity: a review. Chem Eng J 2016;283:789–805.
[30] Savage PE. Organic chemical reactions in supercritical water. Chem Rev 1999;99:603–22.
[31] Marcus Y. On transport properties of hot liquid and supercritical water and their relationship to the hydrogen bonding. Fluid Phase Equilibria 1999;164:131–42.
[32] Kalinichev AG, Bass JD. Hydrogen bonding in supercritical Water. 2. Computer simulations. J Phys Chem A 1997;101:9720–7.
[33] Ruiz HA, Rodríguez-Jasso RM, Fernandes BD, Vicente AA, Teixeira JA. Hydrothermal processing, as an alternative for upgrading agriculture residues and marine biomass according to the biorefinery concept: a review. Renew Sustain Energy Rev 2013;21:35–51.
[34] Wagner W, P A. The IAPWS formulation 1995 for the Thermodynamic properties of ordinary water substance for general and scientific use. J Phys Chem 2002;31:149.
[35] Silveira MHL, Morais ARC, da Costa Lopes AM, Olekszyszen DN, Bogel-Łukasik R, Andreaus J, et al. Current pretreatment technologies for the development of cellulosic ethanol and biorefineries. ChemSusChem 2015;8:3366–90.
[36] Gao Y, Wang X-H, Yang H-P, Chen H-P. Characterization of products from hydrothermal treatments of cellulose. Energy 2012;42:457–65.
[37] Lu X, Berge ND. Influence of feedstock chemical composition on product formation and characteristics derived from the hydrothermal carbonization of mixed feedstocks. Bioresour Technol 2014;166:120–31.
[38] Abel S, Peters A, Trinks S, Schonsky H, Facklam M, Wessolek G. Impact of biochar and hydrochar addition on water retention and water repellency of sandy soil. Geoderma 2013;202–203:183–91.
[39] Heilmann SM, Molde JS, Timler JG, Wood BM, Mikula AL, Vozhdayev GV, et al. Phosphorus reclamation through hydrothermal carbonization of animal manures. Environ Sci Technol 2014;48:10323–9.
[40] Erdogan E, Atila B, Mumme J, Reza MT, Toptas A, Elibol M, et al. Characterization of products from hydrothermal carbonization of orange pomace including anaerobic digestibility of process liquor. Bioresour Technol 2015;196:35–42.
[41] Parshetti GK, Chowdhury S, Balasubramanian R. Hydrothermal conversion of urban food waste to chars for removal of textile dyes from contaminated waters. Bioresour Technol 2014;161:310–9.
[42] Berge ND, Ro KS, Mao J, Flora JRV, Chappell MA, Bae S. Hydrothermal carbonization of municipal waste streams. Environ Sci Technol 2011;45:5696–703.
[43] Parshetti GK, Liu Z, Jain A, Srinivasan MP, Balasubramanian R. Hydrothermal carbonization of sewage sludge for energy production with coal. Fuel 2013;111:201–10.
[44] Alatalo S-M, Repo E, Mäkilä E, Salonen J, Vakkilainen E, Sillanpää M. Adsorption behavior of hydrothermally treated municipal sludge & pulp and paper industry sludge. Bioresour Technol 2013;147:71–6.
[45] Du Z, Hu B, Shi A, Ma X, Cheng Y, Chen P, et al. Cultivation of a microalga Chlorella vulgaris using recycled aqueous phase nutrients from hydrothermal carbonization process. Bioresour Technol 2012;126:354–7.
[46] Cao X, Ro KS, Libra JA, Kammann CI, Lima I, Berge N, et al. Effects of biomass types and carbonization conditions on the chemical characteristics of hydrochars. J Agric Food Chem 2013;61:9401–11.
[47] Sun Y, Gao B, Yao Y, Fang J, Zhang M, Zhou Y, et al. Effects of feedstock type, production method, and pyrolysis temperature on biochar and hydrochar properties. Chem Eng J 2014;240:574–8.
[48] Hoekman SK, Broch A, Robbins C, Zielinska B, Felix L. Hydrothermal carbonization (HTC) of selected woody and herbaceous biomass feedstocks. Biomass-Convers Biorefinery 2012;3:113–26.
[49] Möller M, Nilges P, Harnisch F, Schröder U. Subcritical water as reaction environment: fundamentals of hydrothermal biomass transformation. ChemSusChem 2011;4:566–79.
[50] Bobleter O. Hydrothermal degradation of polymers derived from plants. Prog Polym Sci 1994:797–841.
[51] Knezevic WvSaSK D. Hydrothermal conversion of biomass. II. conversion Of wood, pyrolysis oil, And glucose In hot compressed water. Ind Eng Chem Res 2010;49:104–12.
[52] Krevelen DV. Graphical-statistical method for the study of structure and reaction processes of coal. Fuel 1950;29:84.
[53] Sevilla M, Fuertes AB. The production of carbon materials by hydrothermal carbonization of cellulose. Carbon 2009;47:2281–9.
[54] Parshetti GK, Kent Hoekman S, Balasubramanian R. Chemical, structural and combustion characteristics of carbonaceous products obtained by hydrothermal carbonization of palm empty fruit bunches. Bioresour Technol 2013;135:683–9.
[55] Kim D, Lee K, Park KY. Hydrothermal carbonization of anaerobically digested sludge for solid fuel production and energy recovery. Fuel 2014;130:120–5.
[56] Sevilla M, Fuertes AB. Chemical and structural properties of carbonaceous products obtained by hydrothermal carbonization of saccharides. Chem - A Eur J 2009;15:4195–203.
[57] Hwang I-H, Aoyama H, Matsuto T, Nakagishi T, Matsuo T. Recovery of solid fuel from municipal solid waste by hydrothermal treatment using subcritical water. Waste Manag 2012;32:410–6.
[58] Hoekman SK, Broch A, Robbins C. Hydrothermal carbonization (HTC) of lignocellulosic biomass. Energy Fuels 2011;25:1802–10.
[59] Peng C, Zhai Y, Zhu Y, Xu B, Wang T, Li C, et al. Production of char from sewage sludge employing hydrothermal carbonization: char properties, combustion behavior and thermal characteristics. Fuel 2016;176:110–8.
[60] He C, Giannis A, Wang J-Y. Conversion of sewage sludge to clean solid fuel using hydrothermal carbonization: hydrochar fuel characteristics and combustion behavior. Appl Energy 2013;111:257–66.
[61] Kang S, Li X, Fan J, Chang J. Characterization of hydrochars produced by hydrothermal carbonization of lignin, cellulose,D-xylose, and wood meal. Ind Eng Chem Res 2012;51:9023–31.
[62] Gao Y, Wang X, Wang J, Li X, Cheng J, Yang H, et al. Effect of residence time on chemical and structural properties of hydrochar obtained by hydrothermal carbonization of water hyacinth. Energy 2013;58:376–83.
[63] Romero-Anaya AJ, Ouzzine M, Lillo-Ródenas MA, Linares-Solano A. Spherical carbons: synthesis, characterization and activation processes. Carbon 2014;68:296–307.
[64] Falco C, Baccile N, Titirici M-M. Morphological and structural differences between glucose, cellulose and lignocellulosic biomass derived hydrothermal carbons. Green Chem 2011;13:3273.
[65] Y. Zhou YL, Wan C, Li D, Mao Z. Effect of hot water pretreatment severity on the degradation and enzymatic hydrolysis of corn stover. Trans ASABE 2010;53:1929–34.
[66] R. P. Overend EC. Fractionation of lignocellulosics by steam: aqueous pretreatments. Philos Trans R Soc Lond A 1987;321:523–6.
[67] Zhang T, Kumar R, Tsai Y-D, Elander RT, Wyman CE. Xylose yields and relationship to combined severity for dilute acid post-hydrolysis of xylooligomers from hydrothermal pretreatment of corn stover. Green Chem 2015;17:394–403.
[68] Nitsos CK, Choli-Papadopoulou T, Matis KA, Triantafyllidis KS. Optimization of hydrothermal pretreatment of hardwood and softwood lignocellulosic residues for selective hemicellulose recovery and improved cellulose enzymatic hydrolysis. ACS Sustain Chem Eng 2016;4:4529–44.
[69] Zakaria MR, Hirata S, Fujimoto S, Hassan MA. Combined pretreatment with hot compressed water and wet disk milling opened up oil palm biomass structure resulting in enhanced enzymatic digestibility. Bioresour Technol 2015;193:128–34.
[70] Zakaria MR, Hirata S, Hassan MA. Hydrothermal pretreatment enhanced enzymatic hydrolysis and glucose production from oil palm biomass. Bioresour Technol 2015;176:142–8.
[71] Díaz MJ, Cara C, Ruiz E, Romero I, Moya M, Castro E. Hydrothermal pre-treatment of rapeseed straw. Bioresour Technol 2010;101:2428–35.
[72] Muangrat R, Onwudili JA, Williams PT. Influence of alkali catalysts on the production of hydrogen-rich gas from the hydrothermal gasification of food processing waste. Appl Catal B: Environ 2010;100:440–9.

[73] Wang T, Zhai Y, Zhu Y, Peng C, Xu B, Wang T, et al. Acetic acid and sodium hydroxide-aided hydrothermal carbonization of woody biomass for enhanced pelletization and fuel properties. Energy Fuels 2017.
[74] Lu X, Flora JRV, Berge ND. Influence of process water quality on hydrothermal carbonization of cellulose. Bioresour Technol 2014;154:229–39.
[75] Reza MT, Rottler E, Herklotz L, Wirth B. Hydrothermal carbonization (HTC) of wheat straw: influence of feedwater pH prepared by acetic acid and potassium hydroxide. Bioresour Technol 2015;182:336–44.
[76] Yang W, Shimanouchi T, Kimura Y. Characterization of the residue and liquid products produced from husks of nuts fromCarya cathayensisSarg by hydrothermal carbonization. ACS Sustain Chem Eng 2015;3:591–8.
[77] Flora JFR, Lu X, Li L, Flora JRV, Berge ND. The effects of alkalinity and acidity of process water and hydrochar washing on the adsorption of atrazine on hydrothermally produced hydrochar. Chemosphere 2013;93:1989–96.
[78] Liang J, Liu Y, Zhang J. Effect of solution pH on the carbon microsphere synthesized by hydrothermal carbonization. Procedia Environ Sci 2011;11:1322–7.
[79] Mäkelä M, Fraikin L, Léonard A, Benavente V, Fullana A. Predicting the drying properties of sludge based on hydrothermal treatment under subcritical conditions. Water Res 2016;91:11–8.
[80] D. Knezevic WVS, Kersten S. Hydrothermal conversion of biomass: I, glucose conversion in hot compressed water. Ind Eng Chem Res 2009;48:13.
[81] Li M, Li W, Liu S. Hydrothermal synthesis, characterization, and KOH activation of carbon spheres from glucose. Carbohydr Res 2011;346:999–1004.
[82] Zhang B, von Keitz M, Valentas K. Thermochemical liquefaction of high-diversity grassland perennials. J Anal Appl Pyrolysis 2009;84:18–24.
[83] Zhang B, von Keitz M, Valentas K. Thermal effects on hydrothermal biomass liquefaction. Appl Biochem Biotechnol 2008;147:143–50.
[84] Akhtar J, Saidina Amin N. A review on operating parameters for optimum liquid oil yield in biomass pyrolysis. Renew Sustain Energy Rev 2012;16:5101–9.
[85] Brand S, Hardi F, Kim J, Suh DJ. Effect of heating rate on biomass liquefaction: differences between subcritical water and supercritical ethanol. Energy 2014;68:420–7.
[86] Fengel D, Wegener G. Wood: Chemistry, Ultrastructure, Reactions; 1984.
[87] Laureano-Perez L, Teymouri F, Alizadeh H, Dale BE. Understanding factors that limit enzymatic hydrolysis of biomass. Appl Biochem Biotechnol 2005:1081–99.
[88] Mitsuru Sasaki ZF, Fukushima Yoshiko, Adschiri Tadafumi, Arai Kunio. Dissolution and hydrolysis of cellulose in subcritical and supercritical water. Ind Eng Chem Res 2000.
[89] Kumar S. Sub- and supercritical water technology for biofuels. Adv Biofuels Bioprod 2013:147–83.
[90] C. Falco NB, Titirici M-M. Morphological and structural differences between glucose, cellulose and lignocellulosic biomass derived hydrothermal carbons. Green Chem 2011;13.
[91] Titirici M-M, Antonietti M, Baccile N. Hydrothermal carbon from biomass: a comparison of the local structure from poly- to monosaccharides and pentoses/hexoses. Green Chem 2008;10:1204.
[92] Baccile N, Laurent G, Babonneau F, Fayon F, Titirici M-M, Antonietti M. Structural characterization of hydrothermal carbon spheres by advanced solid-state MAS13C NMR Investigations. J Phys Chem C 2009;113:9644–54.
[93] C A, Matsumura Y. Formation of tarry material from 5-HMF in subcritical and supercritical water. Ind Eng Chem Res 2009;48:10.
[94] Falco C, Perez Caballero F, Babonneau F, Gervais C, Laurent G, Titirici M-M, et al. Hydrothermal carbon from biomass: structural differences between hydrothermal and pyrolyzed carbons via13C solid state NMR. langmuir 2011;27:14460–71.
[95] Jun-Li Ren R-CS. Chapter 4 – Hemicelluloses,Cereal Straw as a Resource for Sustainable Biomaterials and Biofuels. Amsterdam: Elsevier; 2010. p. 73–130.
[96] Jing Q, Lü X. Kinetics of non-catalyzed decomposition of D-xylose in high temperature liquid water. Chin J Chem Eng 2007;15:666–9.
[97] Paksung N, Matsumura Y. Decomposition of xylose in sub- and supercritical water. Ind Eng Chem Res 2015;54:7604–13.
[98] Wahyudiono Sasaki M, Goto M. Conversion of biomass model compound under hydrothermal conditions using batch reactor. Fuel 2009;88:1656–64.
[99] Wahyudiono Kanetake T, Sasaki M, Goto M. Decomposition of a lignin model compound under hydrothermal conditions. Chem Eng Technol 2007;30:1113–22.
[100] Besse X, Schuurman Y, Guilhaume N. Hydrothermal conversion of lignin model compound eugenol. Catal Today 2015;258:270–5.
[101] Barbier J, Charon N, Dupassieux N, Loppinet-Serani A, Mahé L, Ponthus J, et al. Hydrothermal conversion of lignin compounds. A detailed study of fragmentation and condensation reaction pathways. Biomass- Bioenergy 2012;46:479–91.
[102] Penninger JMLKR, Baur HCL. Reactions of diphenylether in supercritical water e mechanism and kinetics. J Supercrit Fluids 1999;16:119–32.
[103] M. Saisu TS, Watanabe M, Adschiri T, Arai K, Arai K. Conversion of lignin with supercritical water-phenol mixtures. Energy Fuels 2003.
[104] Fang Z, Sato T, Smith RL, Inomata H, Arai K, Kozinski JA. Reaction chemistry and phase behavior of lignin in high-temperature and supercritical water. Bioresour Technol 2008;99:3424–30.
[105] Bobleter C. Hydrothermal degradation of polymers derived from plants. Prog Polym Sci 1994;19:797–841.
[106] Zhang B, Huang H-J, Ramaswamy S. Reaction kinetics of the hydrothermal treatment of lignin. Appl Biochem Biotechnol 2007;147:119–31.
[107] Hsu T-C, Guo G-L, Chen W-H, Hwang W-S. Effect of dilute acid pretreatment of rice straw on structural properties and enzymatic hydrolysis. Bioresour Technol 2010;101:4907–13.
[108] Anjum M, Khalid A, Mahmood T, Aziz I. Anaerobic co-digestion of catering waste with partially pretreated lignocellulosic crop residues. J Clean Prod 2016;117:56–63.
[109] Rémond C, Aubry N, Crônier D, Noël S, Martel F, Roge B, et al. Combination of ammonia and xylanase pretreatments: impact on enzymatic xylan and cellulose recovery from wheat straw. Bioresour Technol 2010;101:6712–7.
[110] Chen W-H, Pen B-L, Yu C-T, Hwang W-S. Pretreatment efficiency and structural characterization of rice straw by an integrated process of dilute-acid and steam explosion for bioethanol production. Bioresour Technol 2011;102:2916–24.
[111] Ewanick S, Bura R. Hydrothermal Pretreatment of Lignocellulosic Biomass. 2010. p. 3–23.
[112] L Laureano-Perez FT, Alizadeh H. Understanding factors that limit enzymatic hydrolysis of biomass. Appl Biochem Biotechnol 2005:121–4.
[113] Gronli MG. A theoretical and experimental study of the thermal degradation of biomass. Nor Univ Sci Technol 1996:115.
[114] Li Hongjia, Pu Yunqiao, K R, Ragauskas Arthur J, Wyman Charles E. Investigation of lignin deposition on cellulose during hydrothermal pretreatment, its effect on cellulose hydrolysis, and underlying mechanisms. Biotechnol Bioeng 2014;111:8.
[115] Kučerová V, Výbohová E, Čaňová I, Ďurkovič J. The effects of both insoluble lignin and the macromolecular traits of cellulose on the content of saccharides within solids during hydrothermal pretreatment of hybrid poplar wood. Ind Crops Prod 2016;91:22–31.
[116] Vogel H. Hydrothermal carbonization –1. Influence of lignin in lignocelluloses. Chem Eng Technol 2011;22:2037–43.
[117] Kruse A, Funke A, Titirici M-M. Hydrothermal conversion of biomass to fuels and energetic materials. Curr Opin Chem Biol 2013;17:515–21.
[118] Zhai Y, Chen H, Xu B, Xiang B, Chen Z, Li C, et al. Influence of sewage sludge-based activated carbon and temperature on the liquefaction of sewage sludge: yield and composition of bio-oil, immobilization and risk assessment of heavy metals. Bioresour Technol 2014;159:72–9.
[119] He C, Chen C-L, Giannis A, Yang Y, Wang J-Y. Hydrothermal gasification of sewage sludge and model compounds for renewable hydrogen production: a review. Renew Sustain Energy Rev 2014;39:1127–42.
[120] Peterson AA, Vogel F, Lachance RP, Fröling M, Antal JMJ, Tester JW. Thermochemical biofuel production in hydrothermal media: a review of sub- and supercritical water technologies. Energy Environ Sci 2008;1:32.
[121] Rogalinski T, Liu K, Albrecht T, Brunner G. Hydrolysis kinetics of biopolymers in subcritical water. J Supercrit Fluids 2008;46:335–41.
[122] Abdelmoez WNT, Yoshida H. Amino acid transformation and decomposition in saturated subcritical water conditions. Ind Eng Chem Res 2007:46.
[123] Klingler D, Berg J, Vogel H. Hydrothermal reactions of alanine and glycine in sub- and supercritical water. J Supercrit Fluids 2007;43:112–9.
[124] Vallentyne JR. Thermal reaction kinetics and transformation products of amino compounds. Geochim Cosmochim 1964;28.
[125] Danso-Boateng E, Shama G, Wheatley AD, Martin SJ, Holdich RG. Hydrothermal carbonisation of sewage sludge: effect of process conditions on product characteristics and methane production. Bioresour Technol 2015;177:318–27.
[126] Shujauddin M, Changi JLF, Mo Na, Savage Phillip E. Hydrothermal reactions of biomolecules relevant for microalgae liquefaction. Ind Eng Chem Res 2015;54:11733–58.
[127] Peterson AA, Lachance, Russell P, Tester Jefferson W. Kinetic evidence of the Maillard reaction in hydrothermal biomass processing: glucose-glycine interactions in high-temperature, high-pressure water. Ind Eng Chem Res 2010;49:2107–17.
[128] S Inoue SS, Dote Y, Ogi T. Behaviour of nitrogen during liquefaction of dewatered sewage sludge. Biomass- Bioenergy 1997;12:473.
[129] He C, Wang K, Yang Y, Amaniampong PN, Wang J-Y. Effective nitrogen removal and recovery from dewatered sewage sludge using a novel integrated system of accelerated hydrothermal deamination and air stripping. Environ Sci Technol 2015;49:6872–80.
[130] Baccile N, Laurent G, Coelho C, Babonneau F, Zhao L, Titirici M-M. Structural insights on nitrogen-containing hydrothermal carbon using solid-state magic angle spinning13C and15N nuclear magnetic resonance. J Phys Chem C 2011;115:8976–82.
[131] Sevilla M, Gu W, Falco C, Titirici MM, Fuertes AB, Yushin G. Hydrothermal synthesis of microalgae-derived microporous carbons for electrochemical capacitors. J Power Sources 2014;267:26–32.
[132] Falco C, Sevilla M, White RJ, Rothe R, Titirici M-M. Renewable nitrogen-doped hydrothermal carbons derived from microalgae. ChemSusChem 2012;5:1834–40.
[133] Xu ZFaC. Near-critical and Supercritical water and their applications for biorefineries. Biofuels and Biorefineries 2014;2.
[134] Liu Z, Quek A, Kent Hoekman S, Balasubramanian R. Production of solid biochar fuel from waste biomass by hydrothermal carbonization. Fuel 2013;103:943–9.
[135] Tekin K, Karagöz S, Bektaş S. A review of hydrothermal biomass processing. Renew Sustain Energy Rev 2014;40:673–87.
[136] vK DW. Graphical statistical method for the study of structure and reaction processes of coal. Fuel 1950;29.
[137] Ma D, Zhang G, Zhao P, Areeprasert C, Shen Y, Yoshikawa K, et al. Hydrothermal treatment of antibiotic mycelial dreg: more understanding from fuel characteristics. Chem Eng J 2015;273:147–55.
[138] Kambo HS, Dutta A. Strength, storage, and combustion characteristics of densified lignocellulosic biomass produced via torrefaction and hydrothermal carbonization. Appl Energy 2014;135:182–91.
[139] Novianti S, Biddinika MK, Prawisudha P, Yoshikawa K. Upgrading of palm oil empty fruit bunch employing hydrothermal treatment in lab-scale and pilot scale. Procedia Environ Sci 2014;20:46–54.
[140] Lucia Calucci DPR, Forte Claudia. Solid-state nuclear magnetic resonance characterization of chars obtained from hydrothermal carbonization of Corncob and Miscanthus. Energy Fuels 2012;27:7.

[141] Xiao L-P, Shi Z-J, Xu F, Sun R-C. Hydrothermal carbonization of lignocellulosic biomass. Bioresour Technol 2012;118:619–23.
[142] Zhang L, Wang Q, Wang B, Yang G, Lucia LA, Chen J. Hydrothermal carbonization of Corncob residues for hydrochar production. Energy Fuels 2015. [150112093612000].
[143] Yao Z, Ma X. Characteristics of co-hydrothermal carbonization on polyvinyl chloride wastes with bamboo. Bioresour Technol 2018;247:302–9.
[144] Zhao P, Chen H, Ge S, Yoshikawa K. Effect of the hydrothermal pretreatment for the reduction of NO emission from sewage sludge combustion. Appl Energy 2013;111:199–205.
[145] Areeprasert C, Zhao P, Ma D, Shen Y, Yoshikawa K. Alternative solid fuel production from paper sludge employing hydrothermal treatment. Energy Fuels 2014;28:1198–206.
[146] Zhuang X, Zhan H, Huang Y, Song Y, Yin X, Wu C. Denitrification and desulphurization of industrial biowastes via hydrothermal modification. Bioresour Technol 2018. http://dx.doi.org/10.1016/j.biortech.2018.01.061.
[147] Calucci L, Rasse DP, Forte C. Solid-state nuclear magnetic resonance characterization of chars obtained from hydrothermal carbonization of Corncob and Miscanthus. Energy Fuels 2013;27:303–9.
[148] Sevilla M, Maciá-Agulló JA, Fuertes AB. Hydrothermal carbonization of biomass as a route for the sequestration of CO_2: chemical and structural properties of the carbonized products. Biomass- Bioenergy 2011;35:3152–9.
[149] Liu Z, Zhang F-S, Wu J. Characterization and application of chars produced from pinewood pyrolysis and hydrothermal treatment. Fuel 2010;89:510–4.
[150] Hu Z, Ragauskas AJ. Hydrothermal pretreatment of switchgrass. Ind Eng Chem Res 2011;50:4225–30.
[151] J-h Zhang, Lin Q-m, Zhao X-r. The hydrochar characters of municipal sewage sludge Under different hydrothermal temperatures and durations. J Integr Agric 2014;13:471–82.
[152] Sabzoi Nizamuddin NM, Tiripathi Manoj, Jayakumar NS, Sahu JN, Ganesan P. Chemical, dielectric and structural characterization of optimized hydrochar produced from hydrothermal carbonization of palm shell. Fuel 2016;163:9.
[153] Marta Sevilla JAM-A, Antonio B Fuertes. Hydrothermal carbonization of biomass as a route for the sequestration of CO_2: chemical and structural properties of the carbonized products. Biomass- Bioenergy 2011;35:7.
[154] Wang L, Li A. Hydrothermal treatment coupled with mechanical expression at increased temperature for excess sludge dewatering: the dewatering performance and the characteristics of products. Water Res 2015;68:291–303.
[155] Chinnathan Areeprasert PDM, Shen Yafei, Yoshikawa Kunio. Alternative solid fuel production from paper sludge employing hydrothermal treatment. Energy fuels 2014;28:9.
[156] Yan Zhao SZ, Chen Jiajun. Mechanisms of sequential dissolution and hydrolysis for lignocellulosic waste using a multilevel hydrothermal process. Chem Eng J 2015;273:9.
[157] Liu F, Guo M. Comparison of the characteristics of hydrothermal carbons derived from holocellulose and crude biomass. J Mater Sci 2014;50:1624–31.
[158] Linghui YuCF, Weber Jens, White Robin J, Howe Jane Y, Titirici Maria-Magdalena. Carbohydrate-derived hydrothermal carbons: a Thorough characterization study. Langmuir 2012;28:11.
[159] Pin Gao AYZ, Meng Fang, Zhang Yihui, Liu Zhenhong, Zhang Wenqi, Xue Gang. Preparation and characterization of hydrochar from waste eucalyptus bark by hydrothermal carbonization. Energy 2016;97:8.
[160] Liu Zhengang RB. Upgrading of waste biomass by hydrothermal carbonization (HTC) and low temperature pyrolysis (LTP): a comparative evaluation. Appl Energy 2014;114:8.
[161] Liu Z, Balasubramanian R. Upgrading of waste biomass by hydrothermal carbonization (HTC) and low temperature pyrolysis (LTP): a comparative evaluation. Appl Energy 2014;114:857–64.
[162] Manyà JJ. Pyrolysis for Biochar purposes: a Review to establish current knowledge gaps and research needs. Environ Sci Technol 2012;46:7939–54.
[163] He C, Zhao J, Yang Y, Wang J-Y. Multiscale characteristics dynamics of hydrochar from hydrothermal conversion of sewage sludge under sub- and near-critical water. Bioresour Technol 2016;211:486–93.
[164] Sharma RK, Wooten JB, Baliga VL, Lin X, Geoffrey Chan W, Hajaligol MR. Characterization of chars from pyrolysis of lignin. Fuel 2004;83:1469–82.
[165] Fuertes AB, Arbestain MC, Sevilla M, Maciá-Agulló JA, Fiol S, López R, et al. Chemical and structural properties of carbonaceous products obtained by pyrolysis and hydrothermal carbonisation of corn stover. Aust J Soil Res 2010;48:618.
[166] Nonaka M, Hirajima T, Sasaki K. Upgrading of low rank coal and woody biomass mixture by hydrothermal treatment. Fuel 2011;90:2578–84.
[167] Gai C, Guo Y, Liu T, Peng N, Liu Z. Hydrogen-rich gas production by steam gasification of hydrochar derived from sewage sludge. Int J Hydrog Energy 2016;41:3363–72.
[168] Zhai Y, Xu B, Zhu Y, Qing R, Peng C, Wang T, et al. Nitrogen-doped porous carbon from Camellia oleifera shells with enhanced electrochemical performance. Mater Sci Eng: C 2016;61:449–56.
[169] González JF, Román S, Encinar JM, Martínez G. Pyrolysis of various biomass residues and char utilization for the production of activated carbons. J Anal Appl Pyrolysis 2009;85:134–41.
[170] Schimmelpfennig S, Müller C, Grünhage L, Koch C, Biochar Kammann C. hydrochar and uncarbonized feedstock application to permanent grassland—Effects on greenhouse gas emissions and plant growth. Agric, Ecosyst Environ 2014;191:39–52.
[171] George C, Wagner M, Kücke M, Rillig MC. Divergent consequences of hydrochar in the plant–soil system: arbuscular mycorrhiza, nodulation, plant growth and soil aggregation effects. Appl Soil Ecol 2012;59:68–72.
[172] Bargmann I, Rillig MC, Buss W, Kruse A, Kuecke M. Hydrochar and Biochar effects on germination of Spring Barley. J Agron Crop Sci 2013;199:360–73.
[173] Fang J, Gao B, Chen J, Zimmerman AR. Hydrochars derived from plant biomass under various conditions: characterization and potential applications and impacts. Chem Eng J 2015;267:253–9.
[174] Gajić A, Koch H-J. Sugar Beet (L.) growth reduction caused by hydrochar is related to nitrogen supply. J Environ Qual 2012;41:1067.
[175] Bargmann I, Rillig MC, Kruse A, Greef J-M, Kücke M. Effects of hydrochar application on the dynamics of soluble nitrogen in soils and on plant availability. J Plant Nutr Soil Sci 2014;177:48–58.
[176] Danso-Boateng E, Holdich RG, Martin SJ, Shama G, Wheatley AD. Process energetics for the hydrothermal carbonisation of human faecal wastes. Energy Convers Manag 2015;105:1115–24.
[177] Parshetti GK, Quek A, Betha R, Balasubramanian R. TGA–FTIR investigation of co-combustion characteristics of blends of hydrothermally carbonized oil palm biomass (EFB) and coal. Fuel Process Technol 2014;118:228–34.
[178] Zhai Y, Peng C, Xu B, Wang T, Li C, Zeng G, et al. Hydrothermal carbonisation of sewage sludge for char production with different waste biomass: effects of reaction temperature and energy recycling. Energy 2017;127:167–74.
[179] B. Wirth GE, Lotze-Campen H, Erlach B, Rolinski S, Rothe P. Hydrothermal carbonization: influence of plant capacity, feedstock choice and location on product cost. In: Proceedings of the 19th European Biomass Conference and Exhibition, 6-10 June 2011, Berlin, Germany:2001–2010; 2011.
[180] Tri Sesilia Safril BIS, Yoshikawa Kunio. Commercial demonstration of solid fuel production from municipal solid waste employing the hydrothermal treatment. Int J Environ Sci 2017;2:316–23.